ISTANBUL TECHNICAL UNIVERSITY ★ GRADUATE SCHOOL OF SCIENCE
ENGINEERING AND TECHNOLOGY

MODELLING, SIMULATION AND CONTROL OF A POWERTRAIN WITH DUAL CLUTCH TRANSMISSION

M.Sc. THESIS

Özgün BALCI

Department of Mechanical Engineering

Automotive Programme

MAY 2015

ISTANBUL TECHNICAL UNIVERSITY ★ GRADUATE SCHOOL OF SCIENCE
ENGINEERING AND TECHNOLOGY

MODELLING, SIMULATION AND CONTROL OF A POWERTRAIN WITH DUAL CLUTCH TRANSMISSION

M.Sc. THESIS

Özgün BALCI
503121717

Department of Mechanical Engineering

Automotive Programme

Thesis Advisor: Dr. Orhan ATABAY

MAY 2015

İSTANBUL TEKNİK ÜNİVERSİTESİ ★ FEN BİLİMLERİ ENSTİTÜSÜ

ÇİFT KAVRAMA ŞANZIMANLI GÜÇ AKTARMA SİSTEMİNİN MODELLENMESİ, SİMULASYONU VE KONTROLÜ

YÜKSEK LİSANS TEZİ

Özgün BALCI
503121717

Makine Mühendisliği Anabilim Dalı

Otomotiv Programı

Tez Danışmanı: Dr. Orhan ATABAY

MAYIS 2015

Özgün BALCI, a M.Sc. student of ITU Graduate School of Science Engineering and Technology student ID 503121717, successfully defended the thesis entitled “MODELLING, SIMULATION AND CONTROL OF A POWERTRAIN WITH DUAL CLUTCH TRANSMISSION”, which he prepared after fulfilling the requirements specified in the associated legislations, before the jury whose signatures are below.

Thesis Advisor :	**Dr. Orhan ATABAY** İstanbul Technical University	....
Jury Members :	**Dr. Orhan ATABAY** İstanbul Technical University	....
	Assoc. Prof. Dr. Özgen AKALIN İstanbul Technical University	....
	Asst. Prof. Dr. Tarkan SANDALCI Yıldız Technical University	....

Date of Submission : 4 May 2015
Date of Defense : 27 June 2015

FOREWORD

I am very grateful to Dr. Orhan ATABAY for his excellent supervision, his continuous support and encouragement over the past months. The many inspiring comments that he has provided have been an enormous help in the creation of this thesis.

May 2015

Özgün BALCI
Mechanical Engineer

TABLE OF CONTENTS

Page

ABBREVIATIONS

APP	**:** Accelerator Pedal Position
MVEM	**:** Mean Value Engine Model
DoF	**:** Degrees of Freedom
rpm	**:** Revolution per Mimute
MT	**:** Manual Transmission
AMT	**:** Automated Manual Transmission
AT	**:** Automatic (Conventional Planetary Type) Transmission
CVT	**:** Continiously Variable Transmission
DSG	**:** Direct Shift Gearbox
DCT	**:** Dual Clutch Transmission
PID	**:** Proportional, Integral, Derivative
C1	**:** Clutch 1
C2	**:** Clutch 2
CI	**:** Clutch Input Side
CO	**:** Clutch Output Side
P1	**:** Primary Shaft 1
P2	**:** Primary Shaft 2
S1	**:** Secaondary Shaft 1
S2	**:** Secondary Shaft 2
TCM	**:** Transmission Control Module
HS-CAN	**:** High Speed – Control Area Network

LIST OF TABLES

LIST OF FIGURES

Page

MODELLING, SIMULATION AND CONTROL OF A POWERTRAIN WITH DUAL CLUTCH TRANSMISSION

SUMMARY

In this thesis, a powertrain model, which is equipped with dual clutch transmission, and control strategies are developped on the purpose of using in further control applications. For transmission modeling, mechanical layout of Ford 6DCT250 with dry clutches is adopted.

The model, which is developed in Matlab/Simulink®, is established in a modular approach. 5 Degrees of freedom (DoF) powertrain model (while both of clutches are slipping) is developeded. The model has 4 DoF while one of clutches is engaged (clutch input and output sides are rotating at the same speed).

The model contains 1-D engine map multiplied by the accelerator pedal position (APP) input in order to represent torque production of the engine. Mean value engine model (MVEM) which neglects engine harmonics but still representative especially for shifting control applications.

The transmission module contained detailed friction model of single plate dry dual clutches. The clutch friction model has friction coefficient varied according to slip speed. The clutch and synchronizer actuators are not considered and it is assumed that clutch friction surface normal forces can be controlled directly. Torsional vibration springs, located appropriate positions tangentially, are modelled as spring-damper elements in the powertrain model. Synchronizer model is simplified and not featured with a friction model in contrast to that of clutches. Due to being realized at the torque free half of the transmission, synchronizer changes are represented as a ramp function.

Lateral dynamics of the vehicle such as asymmetrical torque distribution on wheels or cornering are also neglected. This assumption provides the chance of representing half shafts, wheels and forces on them lumped due to symmetric behavior of the differential. In addition to mass feature, half shafts are modeled as spring damper elements due to their length and relatively higher toques applied on them.

Gearshift and synchronizer change timings are determined by the help of a shifting schedule according to instant accelerator pedal position and instant velocity of the vehicle. Shift control is realized by simultaneous clutch normal force control without engine manipulation. During shifting process, clutch control strategies are based on engine speed and clutch slip speed feedbacks (speed based control). Control strategies are defined for launch upshift and downshift separately.

Lastly, the powertrain model is run in three different simulation cycle including various cases in order to investigate the model responses to the control strategies.

Afterwards, the cases are investigated in detail such as engine and primary shafts speed profiles, acceleration characteristics and clutch operations during launch and shifting processes seperately.

ÇİFT KAVRAMA ŞANZIMANLI GÜÇ AKTARMA SİSTEMİNİN MODELLENMESİ, SİMULASYONU VE KONTROLÜ

ÖZET

Bu tezde, çift kavramalı şanzımana sahip bir güç aktarma sistemi modellenmesi, simulasyonu ve kontrolü, daha ileri kontrol uygulamalarında da kullanılmak üzere gerçekleştirilmiştir. Şanzıman modellemesi için kuru kavramalı Ford 6DCT250 mekanik düzeni esas alınmıştır.

Model, Matlab/Simulink® yazılımı kullanılarak modüler bir yaklaşımla oluşturulmuştur. Herhangi bir kavramanın kavranmış olmaması durumunda 5 serbestlik derecesine sahip olan model, bir kavrama kavranmış olduğunda 4 serbestlik derecesine sahiptir. Yay-sönüm elemanları ve sürtünme elemanları matematik modelleme ve simulasyonda hız bilgisini girdi olarak kabul edip tork çıktısı veren elemanlar olarak modellenmiştir. Diğer atalet elemanları içinse bunun tersi geçerlidir.

Bu çalışmanın ilk bölümünde, giriş ve tezin amacı kısmının ardından çift kavramalı şanzıman içeren güç aktarma sistemlerinin matematik modellemesiyle ilgili literatür araştırması sunulmuştur. Ardından güç aktarma sisteminin kısımları; sırasıyla motor, şanzıman, senkromeçler, kavrama ve sürtünme, diferansiyel, tekerlekler, lastik ve taşıtın modellenmesinin literatür taraması ortaya konmuştur. Bu bölümün son kısmında seyir ve vites geçişleri sırasında, vites geçiş zamanlamasının belirlenmesi, kavrama ve senkromeç kumanda sistemlerinin kontrol stratejileri ve motor kontrol stratejileriyle ilgili daha önce yapılmış çalışmalar ele alınmıştır.

Çalışmanın ikinci bölümünde ağırlıklı olarak çift kavramalı şanzımanların genel yapıları ve kullanılan kavrama tür ve tasarımları ve ticari olarak kullanılan farklı şanzıman dizayn ve mekanik düzenleri ve bunun yanında farklı kontrol stratejileri ele alınmıştır.

Üçüncü bölümün ilk kısmında ise bu çalışmada kullanılan güç aktarma sisteminin genel yapısı ve mekanik düzeni belirlenmiştir. Modelde kullanılacak yay-sönüm elemanlarının konumları akışı tespit edilmiştir. Takip eden kısımda motor modeli, kavrama ve sürtünme modeli, statik ve dinamik sürtünme katsayıları karakteristikleri ve ve geçiş mantığı, diferansiyel tekerlek ve lastik modelleri ve taşıt modeli oluşturulmuştur.

Modelde, motor tork üretimini temsilen, gaz pedal pozisyonu (APP) sinyaliyle oranlanmak üzere, bir boyutlu bir motor tork haritası kullanılmıştır. Motor harmonikleri ihmal edilse de kontrol uygulamaları için elverişli olan ortalama değer motor modeli (MVEM) kullanılmıştır. Motordaki ve yataklamalarındaki kayıplar bir

sönüm elemanı kullanılarak temsil edilmiştir. Motor devre bağlı tork karakteristiği iki litre benzinli bir motor karakteristiği örnek alınarak belirlenmiştir.

Şanzıman modulü, detaylı bir tek plakalı kuru kavrama modeli içermektedir. Kavrama sürtünme modeli, kayma hızına bağlı olarak değişen bir sürtünme katsayısı içermektedir. Kavrama ve senkromeç kumanda düzenleri modellemede göz önünde bulundurulmamış, kavrama normal kuvvetlerinin, artış ve azalış hızları sınırlandırılmak şartıyla, direkt olarak kontrol edildiği varsayılmıştır.

Sürtünme plakasına uygun biçimde dairesel olarak yerleştirilmiş, motorda farklı pistonlarda süreksiz ama periyodik olarak meydana gelen yanma sebebiyle oluşan titreşimleri gidermek için kullanılan burulma sönümleyici yaylar, güç aktarma sistem modelinde yay-sönüm elemanları olarak modellenmiştir.

Kavramanın aksine senkromeçler basitleştirilmiş ve sürtünme modeli içermemektedir. Tork akışının olmadığı kısımda gerçekleştirildikleri göz önünde bulundurularak, senkromeç değişimleri matematik modellemede rampa fonksyonu olarak temsil edilmiştir.

Bu çalışmada, tekerlerde asimetrik tork dağılımı ya da viraj gibi araç yanal dinamikleri de ihmal edilmiştir. Bu varsayım, diferansiyelin simetrik davranışına neden olması sayesinde, güç aktarma sisteminde yarım aksları, tekerlekleri ve onlara etkiyen kuvvetleri bir araya toplanmış şekilde modellemeye imkan sunar. Kütle özelliklerinin yanısıra yarım akslar, uzunlukları ve aktardıkları torkun şanzıman elemanlarına görece büyüklüğü nedeniyle yay-sönüm elemanı olarak modellenmişlerdir.

Çalışmanın dördüncü bölümünün başlangıç kısmında vites geçiş zamanlaması ve mantığı tanımlanmış ve vites geçiş haritası oluşturulmuştur. Ardından seyir sırasında tork iletimi olmayan kısımda gerçekleşen vites ön seçimleri zamanlamalarından ve stratejisinden bahsedilmiştir. Daha sonra aracın durağan halden harekete geçtiği kalkış durumunda kavrama kontrol stratejisinden bahsedilmiş, ardından vites geçişleri sırasındaki kavrama normal kuvvet kontrolü stratejileri, tahrikli ve tahriksiz durumlarda, düşük vitese ve tahrikli ve tahriksiz durumlarda yüksek vitese geçişlerde olmak üzere ayrı ayrı ele alınmıştır. Son olarak da senkromeçlerin kontrolü ele alınmıştır.

Vites ve senkromeçlerin değişim zamanlaması vites değişim çizelgesine göre anlık gaz pedalı pozisyonu ve anlık araç hızı değerlerine bağlı olarak gerçekleştirilir. Vites değişim kontrolü, motor tork kontrolü olmadan, eşzamanlı kavrama normal kuvveti kontrolüyle gerçekleştirilir. Kavrama kontrol stratejileri vites değişimi sırasında, motor hızı ve kavrama sürtünme yüzeylerinin kayma hızlarının geribeslemeleriyle gerçekleştirilmektedir. Modelde kalkış prosesi ve tahrikli, tahriksiz durumlarda vites artırma ve vites düşürme ve için farklı kontrol stratejileri tanımlanmış ve simulasyonda denenmiştir.

Bu çalışmanın beşinci bölümünde ise modelin kontrol stratejilerine cevaplarının incelenmesi için güç aktarma sistemi modeli, çeşitli durumlar barındıran üç farklı simulasyon çevriminde koşturulmuştur. Daha sonra, çevrimin kalkış ve vites geçiş süreçlerindeki motor ve vites kutusu giriş mili hız profilleri, ivmelenme karakteristiği, kavrama normal kuvvet kontrolleri ve kayma-kavranma durum geçişleri daha detaylı olarak ayrı ayrı incelenmiştir.

Son olarak, altıncı kısımda, bu çalışmada ve modelde daha ileri düzeyde araştırmalarla yapılabilecek, planlanan ilerlemeler tartışılmış ve fikirler ileri sürülmüştür.

1. INTRODUCTION

Besides comfort and high power generation, improving efficiencies of power generating and transmitting components of a vehicle is one of the main purposes of automotive engineering in order to reduce fuel consumption and emissions.

Due to development of electronics and practicability of control strategies, shifting process optimization by the help of integrated control of engine and transmission, has gained importance for fuel consumption and comfort improvement. For this purpose, various transmission concepts, such as AT (Automatic Transmission), AMT (Automated Manual Transmission), CVT (Continiously Variable Transmission), DCT (Dual Clutch Transmission), have been developed and improved subsequent to conventional manual transmission.

While automatisation of transmissions, in spite of shifting without torque interruption, high losses of AT due to torque convertors, number of friction and one way clutch elements which have been used prevelantly, and in spite of high mechanical efficiency of AMT, torque interrupted shifting consequently low comfort, have caused seeking of new concepts. CVT, which has been developed long ago, has the highest theoretical efficiency by means of possibility of working engine’s most efficient speed permanently. However, that efficiency has never been reached by reason of hydraulic losses, friction problem or high energy expenditure of actuators.

Powertrains equipped with DCT have disadvantage of control difficulties over AT. Hence control strategies of DCT, which possess advantages of shifting capability without torque interruption of AT and high mechanical efficiency of MT at the same time, are critical and open for improvement.

Lessen above mentioned deficiencies of transmission concepts, is a primary aim of automotive area. Modelling and control of automatic transmissions has an important role in order to obtain improvements that will guarantee this high efficiency and comfort characteristics while operating.

1.1 Purpose of Thesis

The purpose of this thesis is to establish a dynamic powertrain model equipped with dual clutch transmission, mean value engine model and detailed clutch model, for the use in gear shift control improvement studies.

The model is expected to possess following characteristics:

• Includes an interpolation of engine map (mean value engine model) which produces representative torque values.

• Contains a detailed dynamic clutch model with a friction coefficient depends on clutch plates' relative velocity.

• Simplified dynamic effects of preselections by syncronisers and neglected reverse gear in order to provide enough simplicity and hence rapidity and low computational requirement

• Establishing a control algorithm that gives reasonable responses.

1.2 Literature Review

In this section, powertrain modelling, in particular modeling studies for dual clutch transmission control applications, will be reviewed. In the first part, powertrain modeling will be discussed in general, namely, modeling tools or the complexity levels of different models in literature such as degrees of freedom, assumptions for simplifications etc. Afterwards, modeling strategies of powertrain components such as engine, clutches, gearboxes, synchronizers, differential, halfshafts, tyres and roadresistance will be considered individually. Finally, clutch and synchronizer actuators and/or engine control strategies will be reviewe.

1.2.1 Powertrain modeling

dip latforms that have been using in powertrain modelling, general structures of the drivetrain, other fundamental principles and approaches will be reviewed in this section.

In powertrain modelling studies, modular approaches, that separates powertrain into simpler elements such as engine, gearbox, syncronizers, differantial, halfshafts (in general as spring-damper elements), tyres and vehicle dynamics, have been adopted prevalently. And these modules are connected to each other via rigid or spring-damper elements. [Goetz 2005] is very comprehensive control study of dual clutch transmission with modular approach. The model was developed in Matlab®/Simulink® simulation platform, containing parts of four cylinder spark ignition engine with airflow dynamics and engine losses, transmission, syncronisers, hydraulic actuation dynamics, differantial, dryshafts, tyres, vehicle dynamics. Equations of motion of the powertrain model were derived by applying Newton's Second Law. This thesis mainly concentrated upon integrated control of shifting proccess with engine manipulation by the help of spark advance control besides that of throttle angle and clutch force. The paper of [Goetz, Levesley and Crolla 2005] also used similar powertrain model, and the main purpose of these studies were to obtain more comfortable shift proccess as against that of planetary-type automatic transmission.

Degree of freedom of a model has a significant importance in terms of optimisation between simplicity, consequently low computational demand, and representativeness of real dynamics of powertrain.

Considering engine output shaft and half shaft as a spring-damper elements is common for such applications. Thereby such powertrains are divided into four different parts by clutches and two spring-damper elements. The paper of (Walker and Zheng 2012) dealt with 15 and 4 degree of freedom powertrain models in order to compare them in terms of their natural modes as response to free vibration analysis. Modal shapes and natural frequencies are identified by the help of eigenvectors and eigenvalues respectively. The paper also compared the effects of harmonical and steady-state engine models which will be further explained in the following section. The study suggested that the four degree of freedom model is capable to yield reasonable results in simulation. Most of studies, that will be mentioned in literature review section of this thesis, treated four degree of freedom models, such as (Kulkarni, Shim and Zhang 2006), (Zhang and Chen 2004), (Liu, Qin, Jiang and Zhang 2009), (Ni, Lu and Zhang 2009) and (Walker, Zhang and Tamba 2007).

In the paper of (Liu, Qin, Jiang and Zhang 2009), a powertrain model is established on the Matlab®/Simulink® platform on the purpose of analysis of both gear shifts and launch proccess. The paper was concentrated on clutch control without consideration of engine manipulation. Control of clutches is realised by the help of PID controller based on engine and clutch speed during launch and torqu phase of shifting. The model and control strategies tested with Ford Motor Co. vehicle for validation. Another model that developed in Matlab®/Simulink® package was adopted in (Ni, Lu and Zhang 2009). A powertrain equiped with dry dual clutch transmission was modeled in order to develop engine and clutch controller to be ensure that these controlled components were tracking desired reference signals.

In the paper of (Kulkarni, Shim and Zhang 2006) a Matlab®/Simulink® model was established, which neglects the delays due to hydraulic actuation system and adds mechanical losses together as vehicle drag. And different launch profiles, in terms of rapidness and comfort characteristics, defined in the study. Another four degree of freedom dual clutch powertrain model is reviewed in the paper of (Walker, Zhang and Tamba 2007). The purpose was improving transient responses of powertrain by the help of integrated control of engine and clutch force. The study also include detailed hydraulic system models.

(Berkel, Hofman, Serrarens and Steinbuch 2013) has a simpler three degree of freedom model. This study mainly concentrate on clutch engagement dynamics, designing and validating a controller. In the paper of (Zhao, Chen, Zhen and Yang 2014) Three degree of freedom model was established on the purpose of develop launch controller involving two clutch simultaneously. The powertrain include six-speed dry dual-clutch transmission. The aim was to distribute friction dissipation, that occurs relatively high during the launch proccess, to the both of clutches instead of first clutch only. Fuzzy logic control strategies were adopted to control clutches. And a linear quadratic regulator was designed in order to optimise clutch control and provide minimum friction wor. The work suggested that this strategies would extend the first clutch’s life span.

Prevalently, dynamic effects of gear preselection have been neglected in control applications of dual clutch transmission. The proccess have been considered limitedly by the reason of occuring out of shifting proccess. In the paper of (Vigliani, Velardocchia and Galvagno 2011) three degrees of freedom transmission model, which also have zero, one degree and two degrees of freedom modes depends on engaged syncroniser number, was established and preselection dynamics were discussed. In this work only the transmission model was developed in

Matlab/Simulink® and studied in order to integrate it other modules (e.g. engine, differantial, wheel).

1.2.2 Engine modeling

In this section, different engine models for modeling and control of dual clutch transmissions are reviewed. Simplified models such as empirical models or lookup tables namely mean engine value models are more common in comparison to harmonic engine models which includes transient response of engine due to discontinuous but periodical firing.

simplified engine models have become popular due to their low complexity and less computational demand. The effect of high frequency engine harmonics is not very considerable for control studies but these harmonics come into prominence clutces' driving and driven plates are about to start to slip while disengagement. In the paper of (Walker, Zheng 2012) these two engine model investigated. Harmonic engine model in this paper included gas cycle, connecting rod and piston inertias which cause a delay in torque transfer from gas cycle to crank shaft. The study suggested that the repeated stick-slips between clutch plates generated by the engine harmonics which are neglecting in mean value engine model may increase torque hole in torque phase of shifting process.

In (Goetz, Levesley, Crolla 2005) adopts a mean value spark ignition engine model which was obtained by neglecting exhaust gas recirculation from (Crossley, Cook 1991) for control application of dual clutch transmission. This model included engine rotational dynamics besides regression function for intake. Airflow dynamics have importance for SI engine models which accept throttle angle and spark advance as inputs and control variables. In (Goetz 2005) similar engine model was used. These models have non-linear relations from experimental data of torque production map of engine depended on engine speed, throttle angle then torque reduction effect of spark advance on torque produced without advance. These models have been modeled in Matlab®/Simulink® platform. Engine accessory loads are coupled to the crankshaft through a common gear ratio.

The paper of (Vigliani, Velardocchia, Galvagno 2011) also made use of stady-stade engine torque map as a function of engine speed and accelerator pedal position namely throttle angle. In this study a transversal engine layout selected. Another simplified engine model is the paper of (Zhao, Chen, Zhen, Yang 2014) which used engine characteristic lookup table for determination of engine torque. Similar lookup table approach reviewed in the paper of (Zhang, Chen 2004) with 3rd order polynomial function of throttle angle and engine speed.

There are several more studies that have used simple mean value engine model in literature, such as (Berkel, Hofman, Serrarens, Steinbuch 2013), (Liu, Qin, Jiang, Zhang 2009), (Ni, Lu, Zhang 2009). Different from those, in (Kulkarni, Shim, Zhang 2006) and (Zhang, Chen 2004) the engine has second spring-damper connection besides input shaft spring-damper elements in order to represent engine mounts.

1.2.3 Transmission modeling

A powertrain mathematical model can be obtained in various ways. The equation of motion can be represented in different forms: In a state space description, including the equation of motion in one set of equations or as a loose set of equations for each single powertrain component from which linear transfer functions may be generated. The latter representation is prevalently used when the model is developed in a modular way (Goetz, 2005).

In modelling studies, different ways can be adopted to derive motion equations. In case of modular approaches, equations of motions often derived by the help of Newton's Second Law.

There exist various DCT mechanical layouts in literature and market. Hence, transmission models differ in their spring-damper elements, torque paths, syncroniser's and clutches locations. Rigid transmission models are generally adopted structures for simpler (lower degrees of freedom) models. However, more detailed transmission models, which have more degrees of freedom, include spring-damper elements such as (Walker and Zheng 2012). The papers of (Goetz 2005) and (Goetz, Levesley and Crolla 2005) studied on a transmission model with different mechanical layout. In this structure clutches have been located separately, which are connected by a connecting shaft. Therefore, the model contains an additional spring-damper element between the first clutch input and the second clutch input besides ones on the primary and secondary shafts of the transmission. In the papers of (Liu, Qin, Jiang and Zhang 2014) and (Jia, Wu and Jia 2013) only primary shafts of transmission were represented as a spring-damper element.

1.2.3.1 Clutch and friction modeling

In the literature, there exists several clutch models, developed in order to represent friction behavior of clutches especially at the vicinity of state changing between engaged and slipping. Namely friction behavior, while relative speeds of clutch input and output plates are very close to zero, is basic focus of clutch modelling.

”Karnopp's model" is one of clutch model which varies order of the friction system while approaching zero relative velocity in order to avoid discontinuity. Another model is the "Reset Integrator Model", which uses spring element to represent linear proportional state of friction at the vicinity of zero velocity. After defined treshold, the model transfers to dynamic friction state. However, in automotive transmission studies, in spite of it’s discontinuity, prevalently unmodified friction models are used which does not allow velocity difference in engaged state in contrast to above models. There only exists a switch logic for transition between static and dynamic states which will be discussed detailed in below sections (Section 3.3).

One of such models in literature is (Goetz 2005) that adopted three order polynomial function on the purpose of representation of dry clutch kinetic friction coefficient pattern based on relative velocity. The thesis also considered effects of lubricant and material of friction plates on kinetic friction behavior. Some of other studies, which defined kinetic friction coefficient based on relative velocity, are (Goetz, Levesley and Crolla 2005), (Zhang and Chen 2004).

Another model of which dynamic friction coefficient is variable, is (Vigliani, Velardocchia and Galvagno 2011). In this paper, for synchroniser modeling, hyperbolic tangent function was adopted in order to reflect dynamic friction coefficient changes due to the relative velocity. Alternatively, the paper of (Kulkarni, Shim and Zhang 2006) clutch friction was modeled as a lookup table of relative velocity and hydraulic force on the clutch spring for simplicity.

In the paper of (Liu, Qin, Jiang, Liu and Zhang 2010) a detailed study on correlation on clutch torque and control parameter was conducted in order to determine torque variation of clutches depends on actuator’s roller position.

1.2.4 Differential and modeling of tyres

Prevalently transmission modeling and control studies have focused on rapid gear shifting provided that longitudinal jerk an energy dissipation of cluthes remain within reasonable bounds. Therefore, lateral dynamics of vehicle in case of cornering or asymmetric torque distribution and angular velocities of tyres can be neglected. Consequently, differential can be considered as a simple gear couple. In literature, this simple differential model is prevalently used for transmission control applications.

In a similar manner, two halfshafts and two tyres are lumped into one element for each in literature. Halfshafts shows spring-damper element properties due to their length and torque that they transmit. Therefore, halfshafts have been modelling as a spring-damper element in most of powertrain modeling studies, such as (Goetz 2005), (Kulkarni, Shim and Zhang 2006), (Ni, Lu and Zhang 2009), (Zhang and Chen 2004) and (Berkel, Hofman, Serrarens and Steinbuch 2013).

As for the tyre model that transmits the torque to the road, rotational dynamics of the tyre are important in terms of powertrain studies. Slip behavior of road contatct surface of the tyre depens on torque transmitted to the road is one of the most important phenomena of the tyre. “Brush” tyre model is a model that can reflect slip behavior. In literature, there exist various models which generate moment between road and tyre depends on slip amount, such as “pacejka tire model” so called “magic formula tire model”, “burckhardt model”, “kiencke & davis model”, “de-wit model” (Jazar 2009) and so on. Also, “rigid ring model”, which neglects slipping and models the tyre as a rigid ring (mass) at outer surface and rotational spring-damper elements between this ring and wheel rim, has been using in order to obtain simplicity. This model provides enough representative dynamics.

1.2.5 Powertrain control

Powertrain control strategies basically aim provide minimum energy dissipation (minimum clutch wear) and maximum comfort and performance, in other words, minimum shift time and minimum jerk. Control, during gearshifts can be implemented locally by use of clutch and syncroniser actuators only. Namely, by taking clutch and syncroniser frictional surfaces normal forces as controlling variables. Also, control can be executed integratedly by the help of engine manipulation during gearshifts additionally, as in the study of (Goetz 2005). The paper of (Walker and Zheng 2012) is another study that use integrated control in order to improve transient response during gearshifts.

Integrated or local control strategies can be investigated in two basic type; “open loop control” is relatively simpler strategy, which consists of preadjusted actuator force look up tables depending on powertrain variables. Such clutch control strategy was used In the paper of (Vigliani, Velardocchia and Galvagno 2011), which investigated transmission kinematics. In case of situations that have not been considered whilst determining of look up tables, clutch control can result in poor response.

Closed loop control strategy determines proper trajectories to be followed for powertrain variables such as enigine speed, engine torque and clutch speed, clutch torque. This control strategy, isolates responses from disturbances.

Closed loop control strategies can also be classified as optimal control or torque based and speed based control in terms of variable that follows a preadjusted trajectory.

In the paper of (Zhao, Jiang, Yu and Zhang 2013), which is mainly focused on launch process control, open loop control strategy was used for determination of clutches’ optimal transfer torque and closed loop control for engine speed or torque trajectory and vhicle shock intensity. These target trajectories determined in consideration of driver intention. The driver intention was reflected by the help of a fuzzy logic with accelerator pedal position and its rate of change inputs. (Zhao, Chen, Zhen and Yang 2014) is another study on launch process with dual clutch transmission. This study propose a launch strategy with both clutches involved simultaneously in order to avoid inequal surface wear of first gear’s clutch. This technique is based on sharing equally of torque by two clutches during launching process in order to extend the service life of twin clutches and separation of the non-target gear clutch by the end of the process. Effect of clutches’ temperatures on friction coefficient is also considered in the model. This study adopted optimal control strategy and took vehicle jerk and clutch surfaces’ friction work as launching quality indices. Engine speed control method was further improved in the study differently from the above study of (Zhao, et al. 2013). Closed-loop control strategy is adopted for the engine in order to obtain three part engine speed pattern, consisting of (1) increasing speed linearly to reduce relative speed between driving and driven plates consequently to reduce friction work, (2) constant engine speed for a short while, (3) accelerating with a linearly icreasing acceleration in the last part of launching to obtain low jerk intensity at the synchronization moment of target clutch. Then PID control is used so as to adapt engine control to driver’s real time behaviours, namely throttle opening.

1.2.5.1 Shift control

Dual clutch transmissions can provide shifts without torque interruption. It is achieved by the help of simultaneous operation of off-going and on-coming gears’ cluthes. Transmitting torque is shared by two clutches during shifting process. Principle torque distribution of DCT is depicted in Figure 1.1.

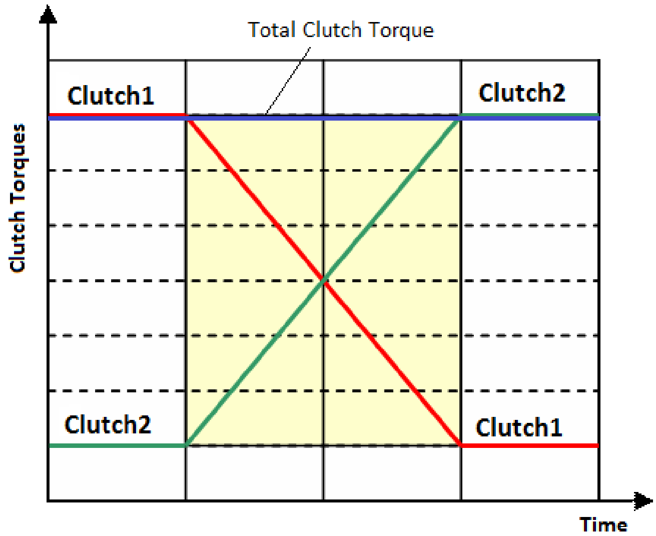

Figure 1.1 : Principle torque distribution of DCT during shift (ZF Getriebe GmbH).

In reality, the torque distribution during shifting is not as stable as that of in principle, due to different kinetic friction coefficient depends on relative speed of surfaces, possible negative friction work on one of clutches (Power cycle) and synchronization process of engine and on-coming clutch speeds after ‘torque phase’, namely, the ‘inertia phase’. In order to overcome these deficits, various strategies have been developed. Figure 1.2 shows effect of torque hole during inertia phase of downshift.

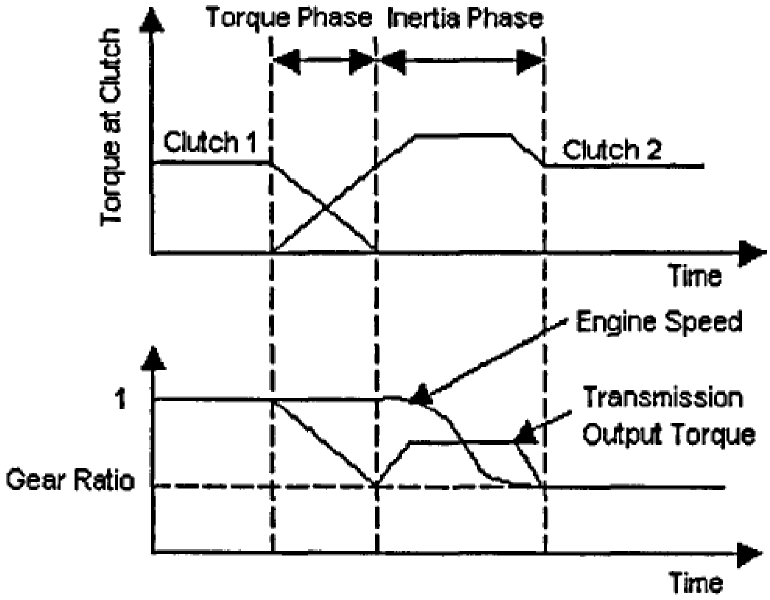

Figure 1.2 : Shift control principle and phases (Goetz 2005).

During an upshift process, in case of early application of on-coming clutch normal force increase, off-going clutch speed may drop below that of engine, before it is entirely disangaged. It causes negative clutch torque on off-going clutch. In order to overcome this problem, in the study of (Goetz 2005), the engine speed was allowed to surpass the off-going clutch speed and held stable until the end of torque phase (off-going clutch is entirely disengaged and entire torque is transmitting via the on-coming clutch). (Liu, Qin, Jiang, Zhang 2014) and (Goetz, Levesley, Crolla 2005) used the same strategy.

The other problem with shifting with DCT is torque hump during inertia phase of upshift or torque hole during inertia phase of downshift due to synchronization of engine speed to on-coming clutch speed. Above figure shows effect of this problem. To treat this problem, engine manipulation is used in the study of (Goetz 2005). During inertia phase of upshift, fuel injection or throttle position is decreased or ignition advance is increased, therefore, engine torque is decreased in order to synchronize the engine speed while clutch transmitting the same torque, and vice versa for downshift process. Off-going clutch is maintained at constant normal force in this phase. Ignition advance control provide relatively quick response in comparison with throttle manipulation but it can also causes increase in emissions. Figure 1.3 depicted clutch slip control during the torque phase and engine manipulation during the inertia phase.

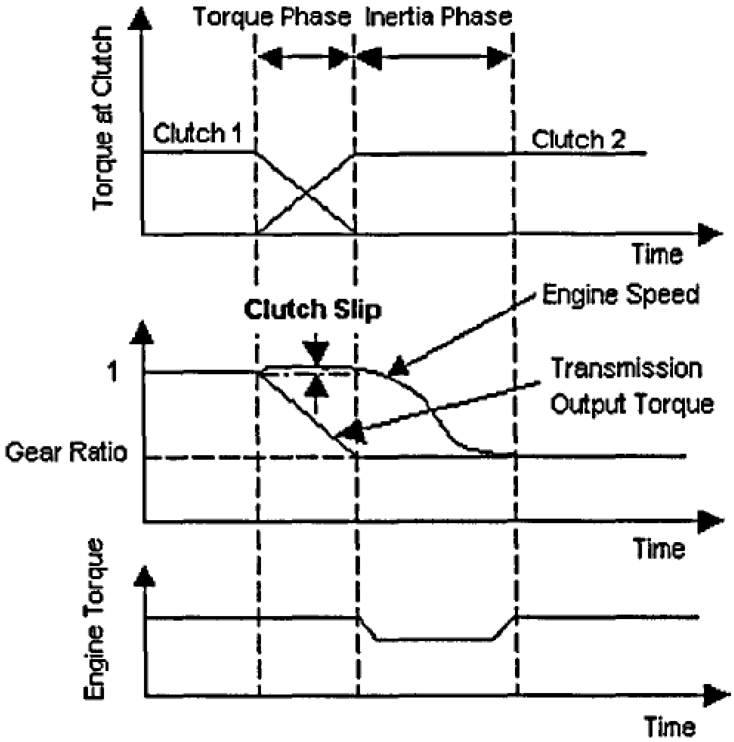

Figure 1.3 : Shift control principle and phases with engine control (Goetz 2005).

Positive speed difference between engine (clutch input) speed and clutch output side of off-going clutch during torque phase provide avoiding negative torque. And torque hump or hole was treated by the help of engine manipulation during inertia phase. The same strategies were used in (Berkel, Hofman, Serrarens, Steinbuch 2013).

1.2.5.2 Gear shift and gear pre-selection

Vehicle speed and accelerator pedal position (APP) data are usually used to determine gear shift schedule. Two main criteria there exist for the schedule; 1) the higher the APP is the higher the vehicle speed for upshift to same gear. 2) There must be hysteresis between speed thresholds to and from any gear, namely, for instance, 2nd to 3rd gear upshift speed threshold is higher than 3rd to 2nd gear downshift speed threshold. These determined schedules are depicted in the studies of (Ni, Lu, Zhang 2009), (Kulkarni, Shim, Zhang 2007).

For gear pre-selection, various strategies there exist. The pre-selection can be executed by means of prediction of the next gear as in (Daimler Chrysler AG 2000 (Patent DE 199 37 716 C1)). It is achieved by taking information of engine and vehicle speeds, accelerator and break pedal positions, and actual gear in any condition of current gear. Another strategy is to keep next lower gear pre-selected for any current gear. This strategy aimed quick response for downshifts, especially in case of hard braking or high torque demand with high accelerator pedal position rate of change. It means, firstly pre-selection of higher gear must be implemented before an upshift and pre-selection of lower gear must be realized after a downshift completed to keep lower gear ready. In this study, this strategy is adopted. A different solution for pre-selection of next gear is not to pre-select any gear at all as in (Volkswagen AG 1998 (Patent DE 196 31 983 C1)). The disadvantage of this strategy is to be obligated to accelerate the torque free shaft in every pre-selection process and hence it extends the pre-selection duration. To solve this problem, before gear shift, target gear speed and synchronizer speed are synchronized by partially engagement of torque free shaft clutch and dog clutches are actuated in order to lock the target gear.

2. GENERAL STRUCTURE OF DUAL CLUTCH TRANSMISSIONS

In this chapter, firstly, general features and principle of DCT will be explained. Then DCTs will be classified in terms of their clutch types and characteristics of these types will be discussed in Section 2.1 Afterwards, various DCT designs produced will be treated in Section 2.2.

The idea of dual clutch transmission is based on the capability of transmitting engine torque through two different ways, which have two independent clutches. One part of transmission drives the odd (1^{st}, 3^{rd}, 5^{th}…) gears and the other one drives the even (2^{nd}, 4^{th}, 6^{th}…) gears. This structure provides shifting without torque interruption by the help of pre-selecting target gear on the torque free half and shift to the target gear involving both of clutches simultaneously.

Each driven disk of clutches is connected to its own shaft and one shaft (solid shaft) is nested in the other (hollow shaft) in order to obtain more compact structure. Principle scheme of a dual clutch transmission is shown in Figure 2.1. These nested shafts are depicted separately to be apparent.

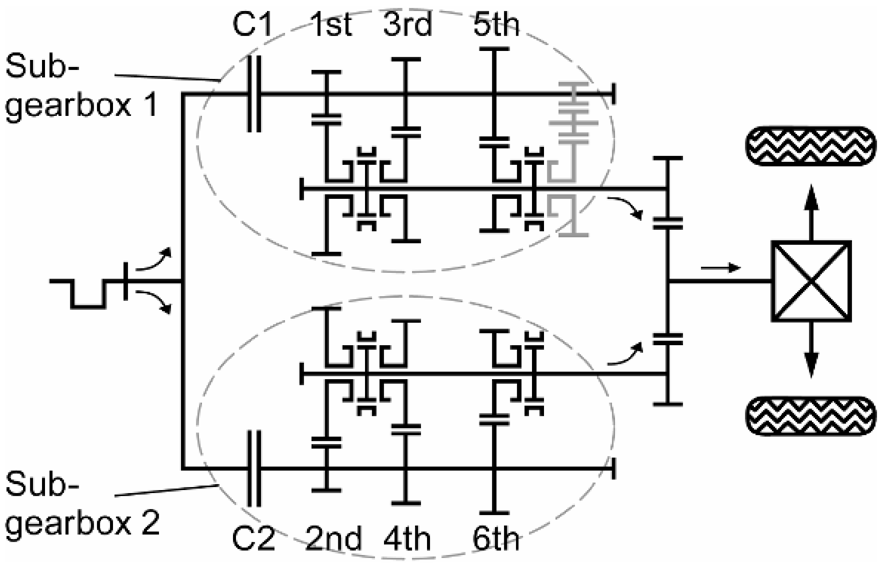

Figure 2.1 : Principle scheme of a powertrain with DCT (Naunheimar et. al. 2011).

Two synchronizers of two different gears on each half can be selected at the same time. The shifting process executed by releasing target gear clutch while actual gear clutch is engaging. During shifting, engine torque is shared by clutches instead of torque interruption. Namely, the oncoming gear clutch torque increases while that of offgoing is decreasing and total torque is not interrupted.

In terms of clutch types, dual clutch transmissions can be classified in two groups as wet and dry.

2.1 DCT Clutch Types

2.1.1 Wet clutches

Wet clutches are designed so as to operate in environment supplied with oil. The main purpose of the oil is serving as a coolant. However, oil has a significant effect on static and kinetic friction coefficient with its viscous friction behavior. The friction coefficient is low in compared to that of dry clutches but has generally positive gradient with clutch surfaces speed difference due to viscous friction.

Wet clutches designed as laminated multi-plate structure. Moment of inertia is still lower in comparison with that of dry clutches due to inexistence of cooling problem. It provides chance to design clutches in more compact smaller and lighter structure. Power capacity that can be transmitted is also not restricted with cooling problem. Therefore wet clutches can be used for heavy vehicles while dry ones usually used for relatively small vehicles due to its low torque capacity. A DSG by VW in a concentric multi-plate wet clutch design is depicted in Figure 2.2 (Naunheimar et. al. 2011).

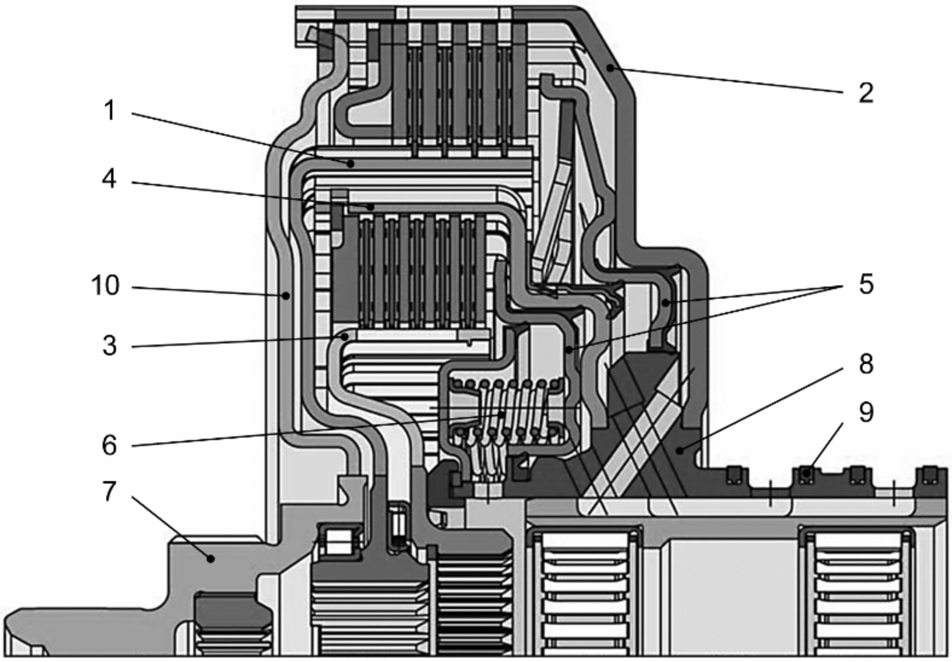

Figure 2.2 : Wet dual clutch of the dual clutch transmission DSG® by VW BorgWarner (Naunheimar et. al. 2011).

Where, 1 is inner plate carrier of the outer clutch, 2 is outer plate carrier of the outer clutch, 3 is inner plate carrier of the inner clutch, 4 is outer plate carrier of the inner clutch, 5 is piston, 6 is compression spring, 7 is input hub, 8 is main hub, 9 is sealing ring and 10 is driving plate

In addition, wet clutches have the advanteges of good controllability, low wear and hence high durability. Since the oil has various function and effects on the system characteristics, oil features and changes in time gain a substantial importance.

Wet dual clutches can be actuated electro-mechanically or electro-hydraulically as well.

2.1.2 Dry clutches

Dry dual clutches transmissions, are usually used in passenger cars with lower engine torques up to 300 Nm approximately, due to their smaller torque capacity.

Dry Dual Clutch Transmissions are usually designed as single clutch plate located between pressure plate and flywheel. Structure of a passenger car single-plate dry clutch by ZF Sachs is shown in Figure 2.3:

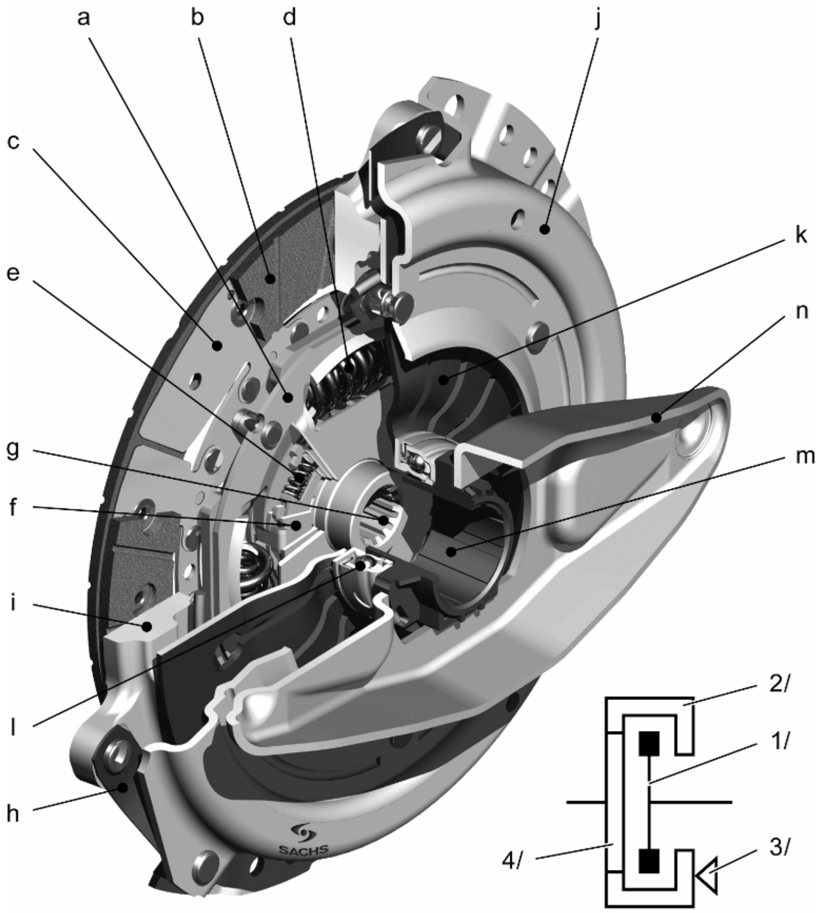

Figure 2.3 : Passenger car single-plate dry clutch by ZF Sachs (Naunheimar et. al. 2011).

Where, 1/ is Clutch plate: a is driving plate, b is friction lining, c is cushion spring, d is torsion spring (driving operation), e is torsion spring (idle operation), f is friction device, g is hub, 2/ is pressure plate assembly: h is return flat spring, i is pressure plate, j is pressure plate housing, k is diaphragm spring, 3/ is clutch actuation: l is release bearing, m is sliding sleeve, n is release lever and 4/ is flywheel.

Due to inexistence of oil between friction surfaces, the friction coefficient is higher than that of wet clutches. However, because of the same reason, control and vibration damping of dry clutches are more critical.

As can be seen in above figure, torsion springs are located on clutch plate on the purpose of damping vibrations result from engine harmonics and friction torque changes. In the assembly two different kinds of torsion springs are located for idle operation and driving conditions. These two sets of sprins cause two damping coefficients each one is effective at different ranges of relative angular displacements. This characteristic curve profile of clutch torsional vibration springs is depicted in the following Figure 2.4:

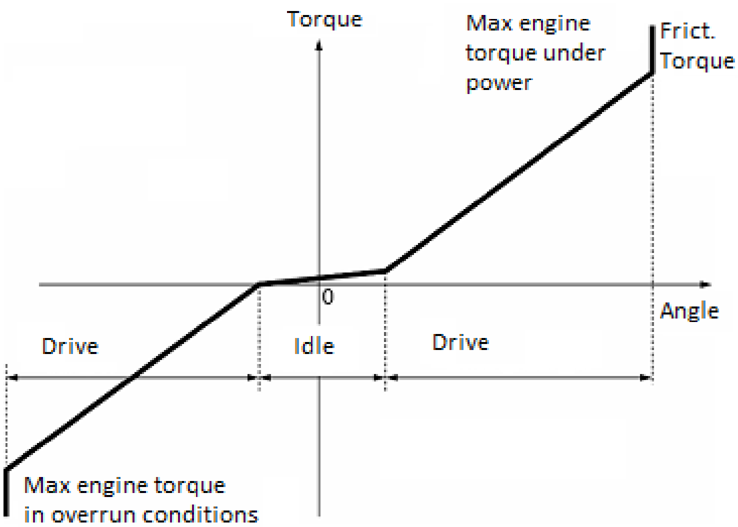

Figure 2.4 : Torsional clutch spring system characteristic curve (Naunheimar et. al. 2011).

The driving damper is adjusted such that, at lowest possible spring stiffness, the friction hysteresis is set which results in the best compromise between resonance damping and degradation of supercritical decoupling. This can help to reduce, for example, rattling noises in the transmission. In order to minimise rattling noises in the transmission when no gear is engaged, the idle damper of the torsional vibration damper is adjusted for idle engine running, the spring stiffness of which is about 1% of the driving damper (Naunheimar et. al. 2011).

Generally, dry clutches equipped with diaphragm springs actuated by electro-mechanically or electro-hydraulically. The normal force on clutch friction surfaces is produced by the actuation of the diaphragm springs. Diaphragm springs have characteristic deflection-force curve which is highly important in terms of clutch control.

Diaphram spring characteristic depends on a set of variable such as material, thickness, outer and inner diameters and height if the spring is designed as truncated cone. The deflection-force profile of the spring for different height-thickness ratios is depicted in Figure 2.5:

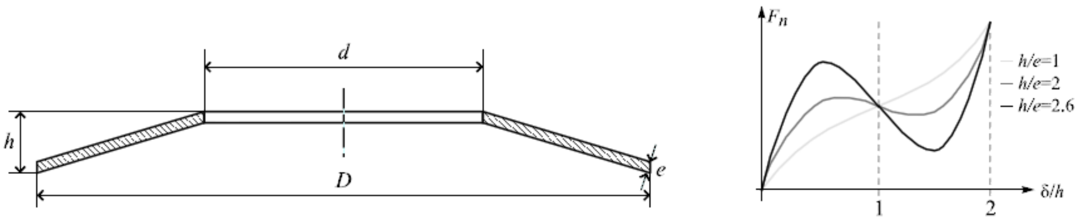

Figure 2.5 : Geometry of a washer spring and its stiffness curve for several h/e ratio (Dolcini et. al. 2009).

Where D is the external and d is the internal diameter of the washer spring, e is the thickness of the washer spring, h height if the truncated cone defined by the unconstrained washer spring, δ the axial deformation of the cone with respect to its unconstrained height.

And another mechanical design of clutch with lever and roller mechanism actuated by electric motor and its characteristic curve is shown in Figure 2.6:

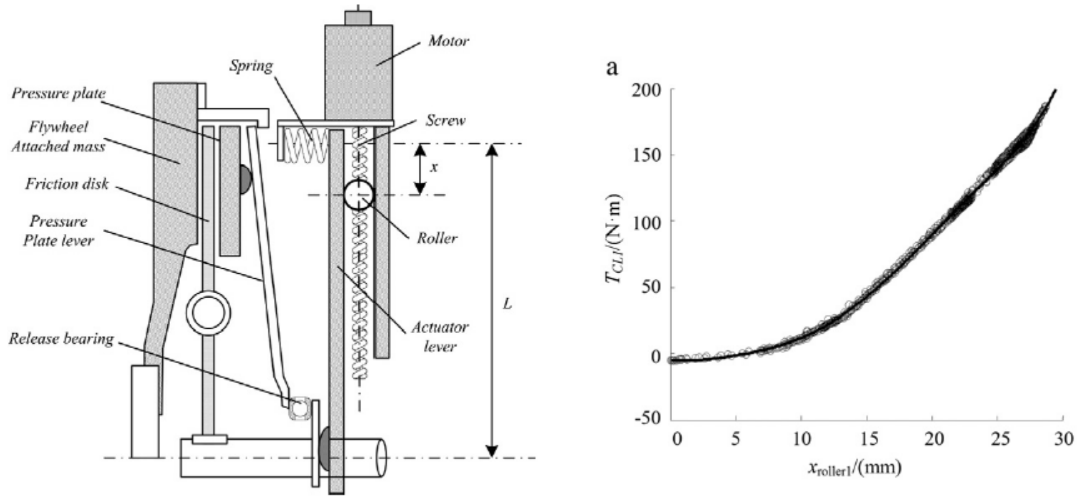

Figure 2.6 : A dual clutch controller structure and its roller displacement-clutch torque curve (Liu et. al. 2014).

The later structure has more linear force curve according to changing effort-weight arms ratios with position of the roller.

2.2 Dual Clutch Transmission Designs

There exist various dual clutch transmission designs with different mechanical layouts. 6-speed front-transverse passenger car DCT VW DSG® with wet running clutches is shown in Figure 2.7 (Naunheimar et. al. 2011).

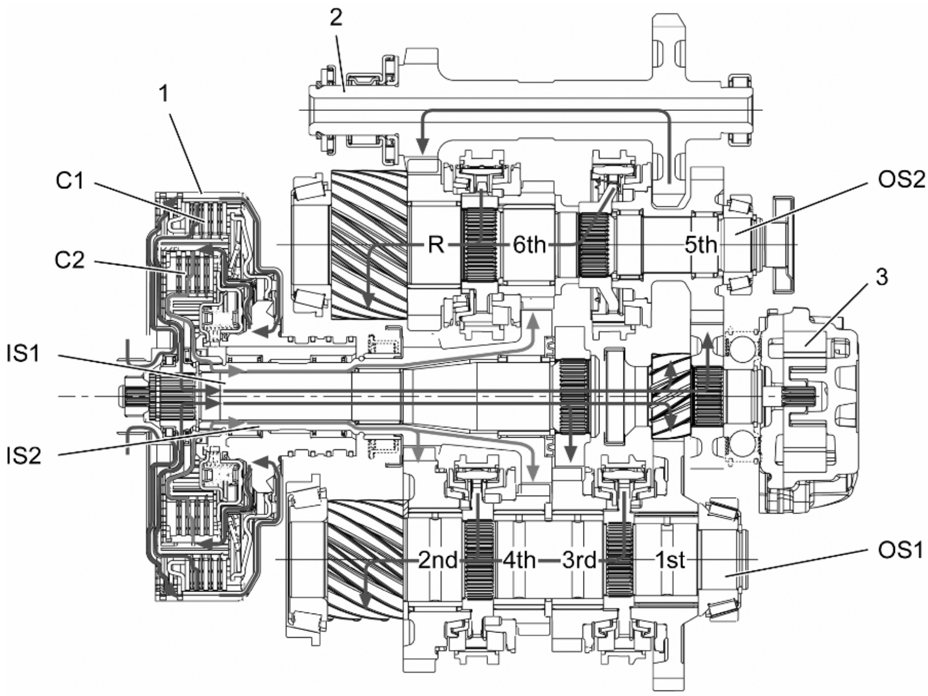

Figure 2.7 : Mechanical layout of 6-speed passenger car DCT VW DSG® (Naunheimar et. al. 2011).

Where, 1 is Wet-running dual clutch with C1 and C2, 2 is reverse idler shaft, 3 is oil pump, IS1 is input shaft of sub-gearbox 1 (1st/3rd/5th/R), IS2 is input shaft of sub-gearbox 2 (2nd/4th/6th), OS1 is output shaft 1 with output constant pinion and OS2 is output shaft 2 with output constant pinion.

The design went into production in 2003. The outer plate carriers of wet running clutches driven by the engine via dual mass flywheel which have high damping capability for engine harmonics and vibration (Naunheimar et. al. 2011). The clutches are also nested as inner and outer. Generally, the outer clutch shows higher performans in comparison to inner one.

As shown in the Figure 2.7, consecutive gears are not necessarily located on different gearbox output shaft differently from principle scheme of DCT. However, consequtive gears must be meshed with gears of different input shaft.

There exist four synchronizers on the gearbox output shafts (secondary shafts). 1st and 3rd, 2nd and 4th, and 6th and reverse gears are combined in terms of synchronizers and 5th gear has its own synchronizer. For the lower gear, multi-cone synchronizers are designed in order to supply high torque requirement due to high gear ratios and synchronization speeds. (Naunheimar et. al. 2011)

The entire design of the same transmission is shown in Figure 2.8:

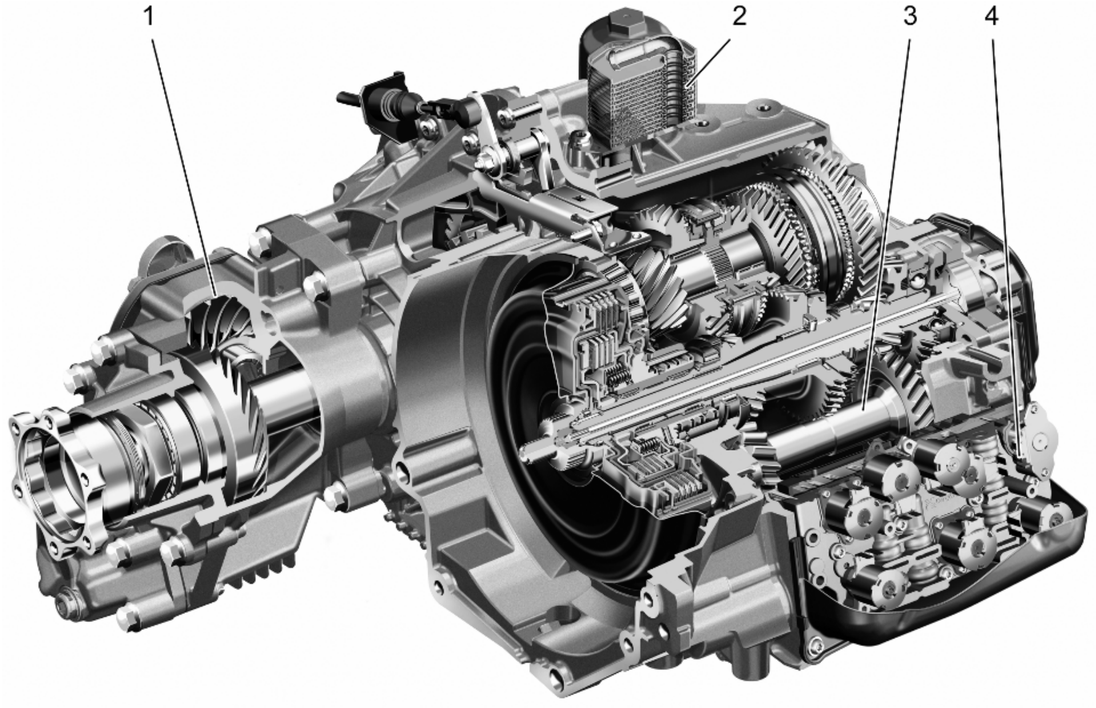

Figure 2.8 : 6-speed passenger car DCT VW DSG® (Naunheimar et. al. 2011).

Where, 1 is Transfer gearbox for all-wheel drive, 2 is oil cooler, 3 is reverse idler shaft and 4 is mechatronic module.

The mechatronic module, which is a local controller connected directly to the vehicle wiring by the help of a central connecter. The module consists of hydraulic module, pressure control valves of clutches, and electronic module with computer and sensor cluster. The system detects gearbox input and gearbox output speeds, actuator positions and temperatures. (Naunheimar et. al. 2011)

Each synchronizer combined with its gear actuator. Volkswagen DSG gear actuators are controlled hydraulically by the help of ball sleeves on both sides. These shift forks' positions can be determined by sensors and magnets. (Naunheimar et. al. 2011)

The hydraulic actuators use pressure oil which is provided by oil pump. This pressure oil also provides clutches cooling by means of oil cooler, seen in Figure 2.8. In addition to its function of protection from wear, gearbox oil has substantial effect on friction coefficient of wet clutches and also on power loss in transmission due to its viscosity and pump efficiency (Naunheimar et. al. 2011).

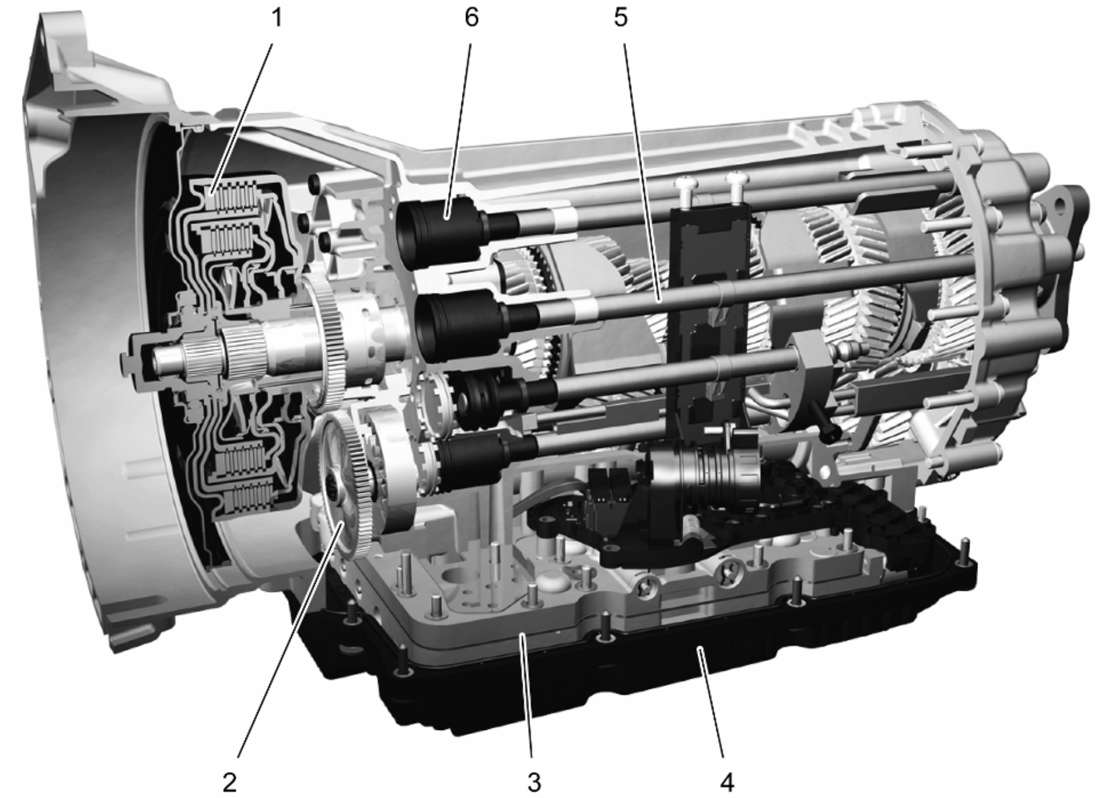

Figure 2.9 : 7-speed passenger car DCT for standard drive ZF 7 DCT 50 (Naunheimar et. al. 2011).

Where, 1 is Dual clutch, 2 is axially parallel oil pump, 3 is hydraulic/mechatronic module, 4 is oil pan, 5 is selector bars and 6 is double-acting shift cylinder.

The 7 DCT 50, 7 speed transmission design by ZF is shown in Figure 2.9. This transmiss went into production in 2005. This transmission also contains dual mass flywheel and wet running clutches. (Naunheimar et. al. 2011)

However the structure of the gearbox design is highly different from the above mentioned Volkswagen design with its two stage axial layout. In this design, there exist only one gear for each gearbox input shaft (primary shaft) and only one gear meshed with these gears to transmit the torque to countershafts. Similarly countershafts are designed one is nested in the other. (Naunheimar et. al. 2011)

Clutches are designed in the same way with VW design that one is nested in the other. The outer clutch is used as standing start element due to its higher performance. In ZF design, inner clutch carriers are designed as continuation of outer carriers differently from above mentioned VW design. This structure provides lower moments of inertia to transmission. (Naunheimar et. al. 2011)

To realize high gearbox efficiency at high engine speeds, an axially parallel pump (2) and injection lubrication are included as further features of this design. The driving gear of oil pump gear stage is directly connected to the outer plate carrier of the clutch rotating with the engine speed (Naunheimar et. al. 2011).

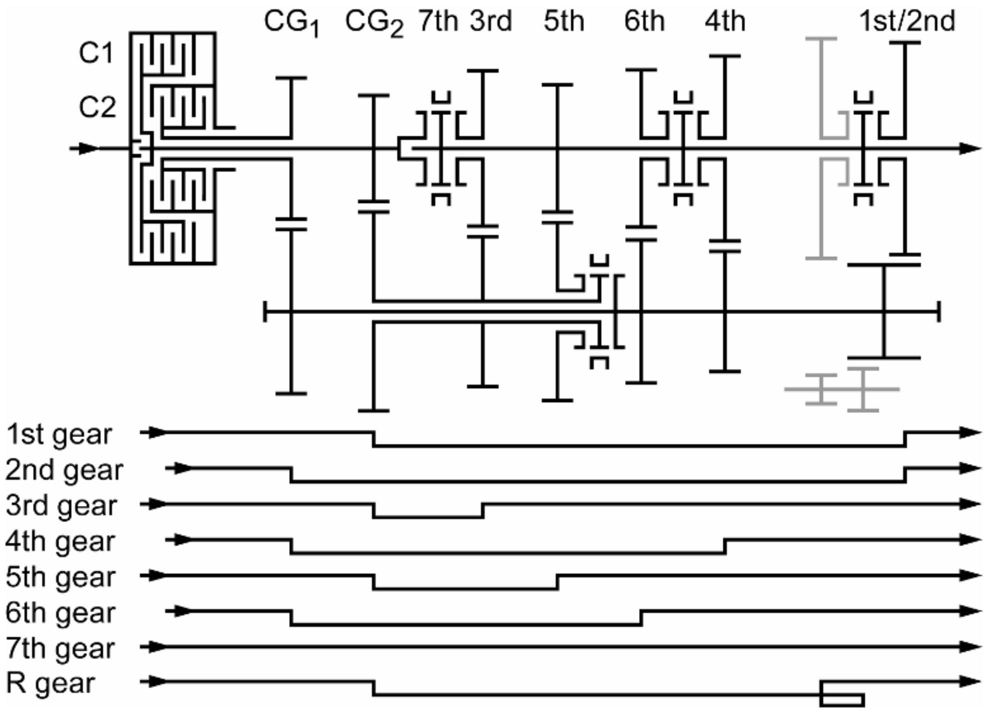

Figure 2.10 : Two-stage 7-speed DCT by ZF (Naunheimar et. al. 2011).

Mechanical layout of the ZF design and power flow paths of gears are depicted in above Figure 2.10. Gear pre-selections are realized by the help of cylinders by electro-hydraulically control of valves and pressure regulators. (Naunheimar et. al. 2011)

As can be seen in Figure 2.10, no pre-selection is required for shifting from 1st to 2nd gear and vice versa. For 7th gear, torque flow is by-passed the countershafts and transmitted to differential with engine speed throughout the outer clutch (C1). Reverse gear is connected to inner countershaft via a pair of gears on an additional countershaft for reverse gear (Naunheimar et. al. 2011).

Another dual clutch transmission design by Ford (6DCT250) with dry clutches is shown in Figure 2.11:

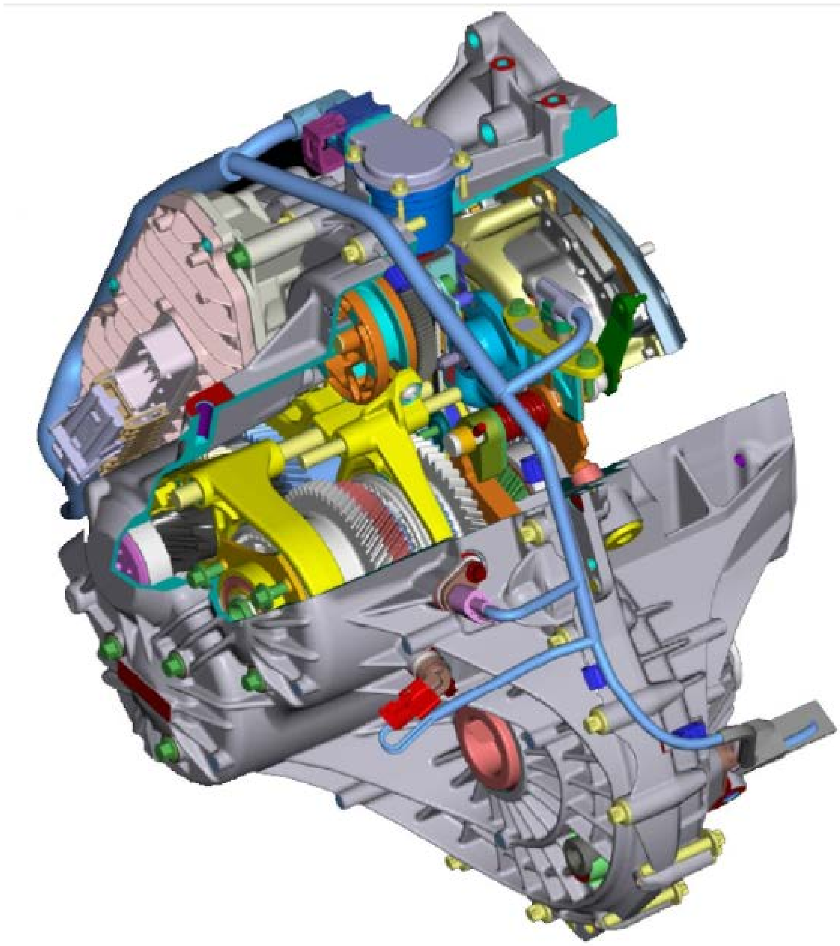

Figure 2.11 : 6 speed DCT (Ford-Werke GmbH).

The transmission is located front transversal on the vehicle. Electro-mechanical actuators are used for gear selection.

The transmission is equipped with dry dual clutches which are designed to reach 250 Nm maximum torque capasity. The mechanical structure of clutches is shown in Figure 2.12:

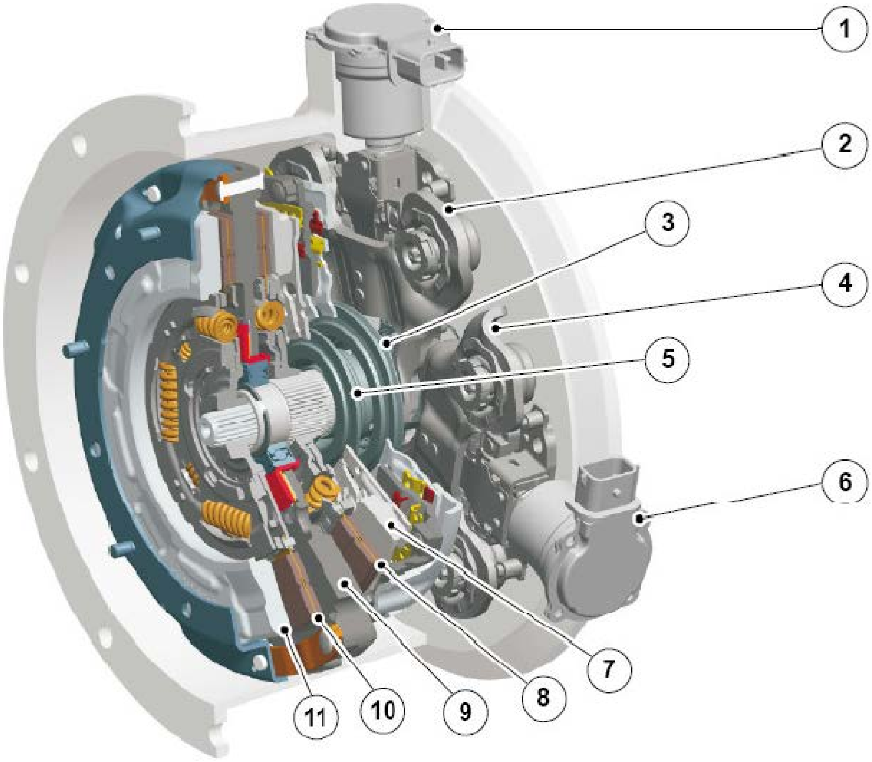

Figure 2.12 : Dry dual clutch module with electro-mechanical actuators (Ford-Werke GmbH).

Where, 1 is electric motor 1 (1^{st}, 3^{rd}, 5^{th} gears), 2 is electro-mechanical actuator 1 (1^{st}, 3^{rd}, 5^{th} gears), 3 is clutch throw-out bearing 1, 4 is electro-mechanical actuator 2 (2^{nd}, 4^{th}, 6^{th}, R gears), 5 is clutch throw-out bearing 2, 6 is electric motor 2 (2^{nd}, 4^{th}, 6^{th}, R gears), 7 is pressure plate 2, 8 is clutch plate 2, 9 is clutch driving disc, 10 is clutch plate 1 and 11 is pressure plate 1.

The clutch plate is located between surfaces of clutch drum and pressure plates driven by the engine via flywheel. Pressure plates are controlled by electro-mechanically by DC motors via a roller moving corresponded to threaded rod and levers design as mentioned before. Axial movement of the roller changes the effort and lever arm ratio and hence normal force on the friction surfaces. When the holding current of DC motor is cut off, the roller is tend to get back to its neutral position due to geometry of the structure. This design provides better controllability and also disengages clutches in case of a failure in the system.

As mentioned before, cooling of clutches is critical for dry DCTs. Clutch temperature is continuously estimated by transmission control module (TCM) with engine torque, signals from gearbox input and output shafts speed sensors and calculated clutch torque. If the calculated temperature surpasses determined critical value, engine torque is reduced and the clutch engagement is realized more rapid and hence shifting duration is reduced in order to avoid any damage due to excessive temperatures.

The torque is transmitted to inner and outer gearbox input shafts via the friction plates. The mechanical layout of 6DCT250 is depicted in Figure 2.13:

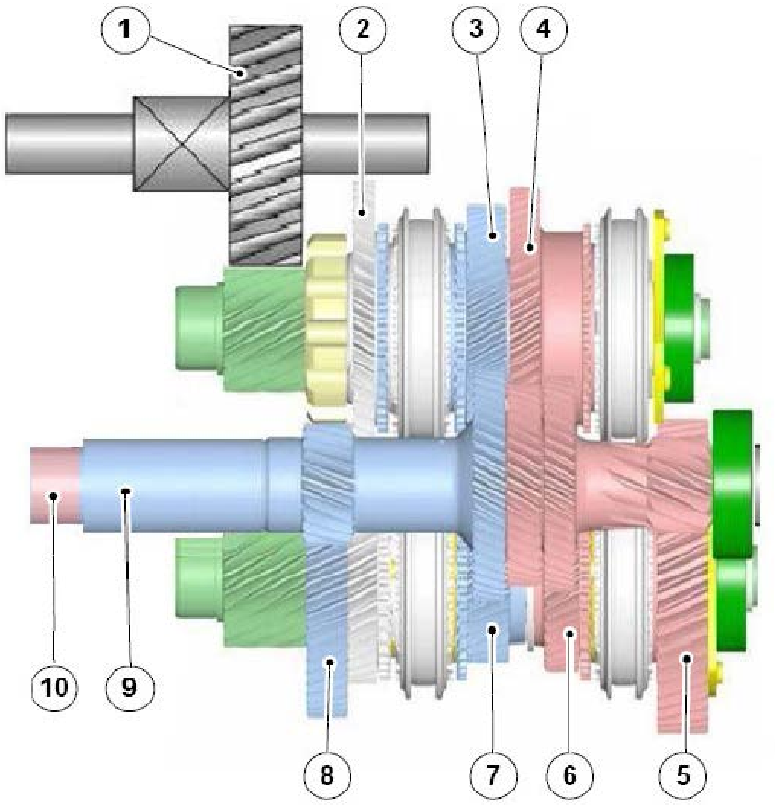

Figure 2.13 : Mechanical layout of a 6 speed DCT (Ford-Werke GmbH).

The 1^{st}, 3^{rd} and 5^{th} gears are connected to inner (solid) gearbox input shaft while the 2^{nd}, 4^{th}, 6^{th} and reverse gears connected to outer (hollow) input shaft. In this design 3rd, 4^{th} and reverse gearwheels are lay on the second gearbox output shaft and 1st, 2^{nd}, 5^{th} and 6^{th} gearwheels are lay on the first output shaft. And four synchronizers are located on the output shafts two for each.

The torque, produced by the engine and conducted to output shafts via the clutches and inner and/or outer shafts is transmited to differential with two different final gear ratios.

The power flow paths of each gear in this design is explained in Figure 2.14:

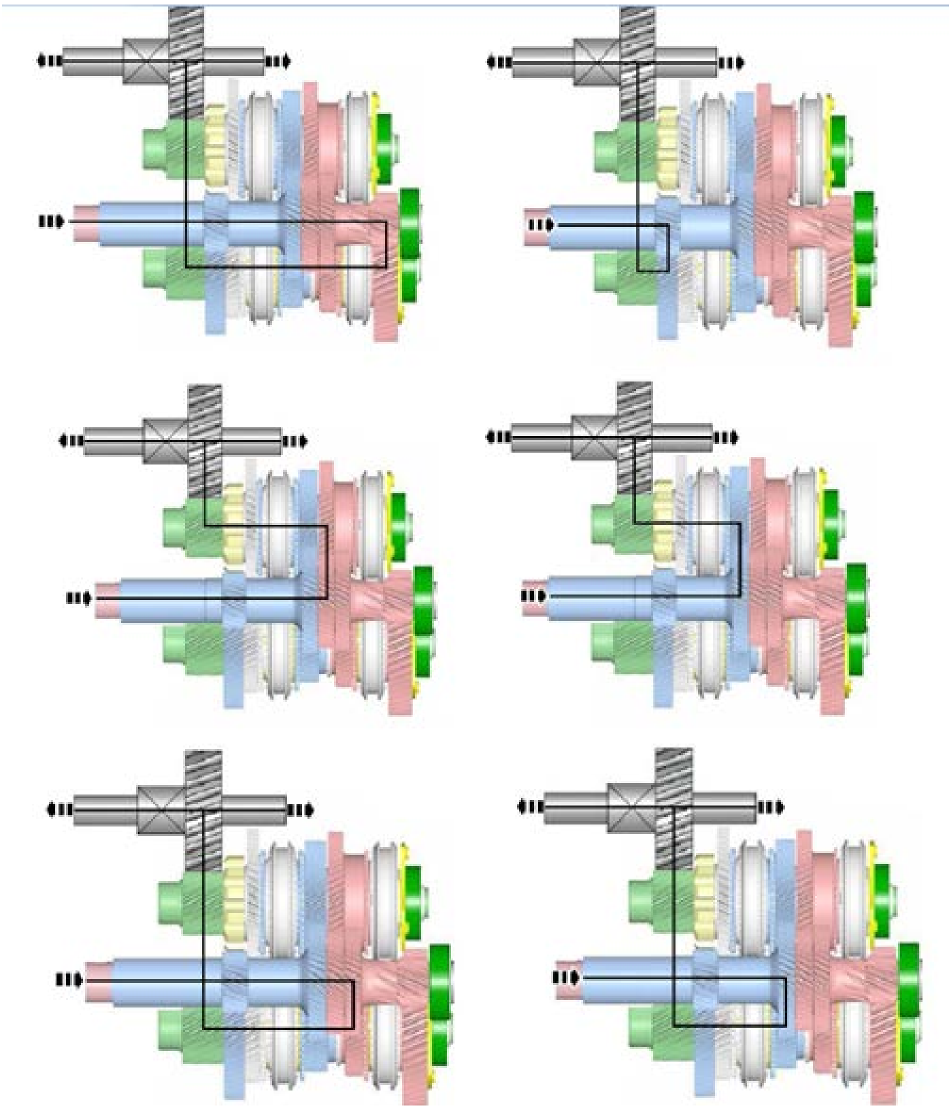

Figure 2.14 : 6 speed DCT power flow paths of each gears (Ford-Werke GmbH).

As can be seen above figure power flows through different input shaft for each consequtive gear.

Gear selection is realized via the synchronizers which are actuated electro-mechanically by two electric motors and two drums with appropriate channels on it. Each drum controls two synchronizers. The gear shifter mechanism is shown in Figure 2.15:

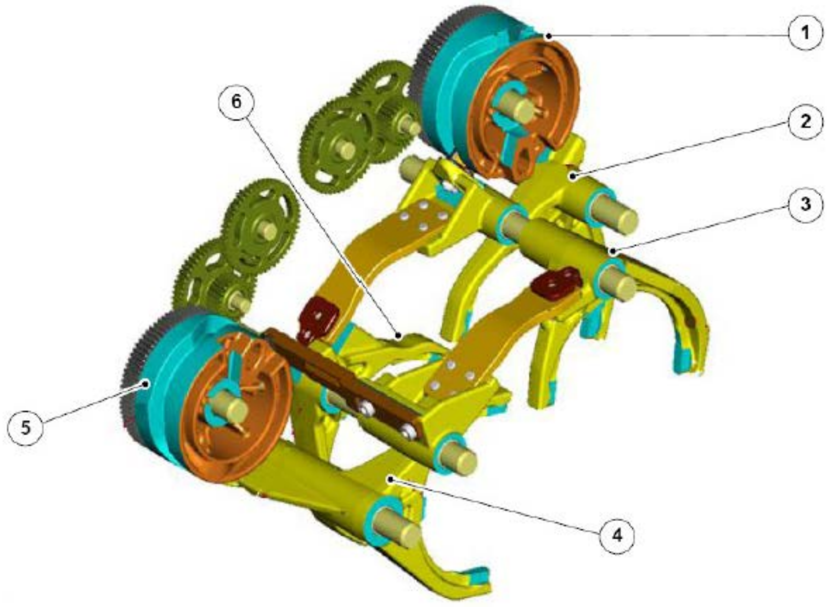

Figure 2.15 : Gear selector system design of a DCT (Ford-Werke GmbH).

Where, 1 is gear selector drum 2, 2 is gear selector housing (R and 4th gear), 3 is gear selector housing (3rd gear), 4 is gear selector housing (1st and 5th gear), 5 is gear selector drum 1 and 6 is gear selector housing (2nd and 6th gear).

As can be seen in the above figure, gear selection is realized via selecting forks controlled by angular position of the drums.

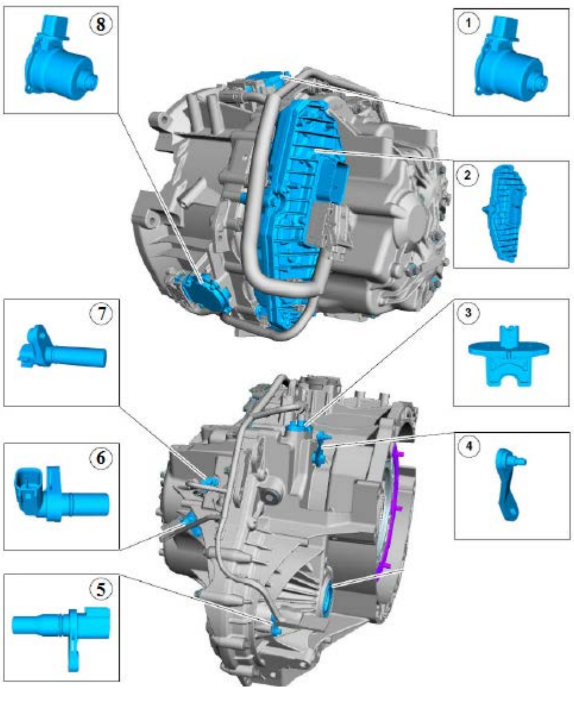

Figure 2.16 : Sensors and actuators of a DCT (Ford-Werke GmbH).

Where, 1 is electric motor 1, 2 is TCM, 3 is gear lever position sensor, 4 is gear shift shaft lever, 5 is output shaft speed sensor, 6 is solid input shaft speed sensor 1, 7 is solid input shaft speed sensor 2 and 8 is electric motor 2.

In the Figure 2.16, sensors, actuators and TCM, which form the transmission control system, are shown.

Gear selecting and shifting process are executed according to various conditions, driver intention and also selected driving mode, such as sport mode, automatic mode, select-shift mode which let the driver to determine gear shifting with some restrictions.

To determine shifting timing, TCM receives various signals via HS-CAN (High Speed Control Area Network). The data that received by TCM are itemized as follows:

• Selected gearshift lever position

• Vehicle speed

• Engine speed, engine torque and acceleration pedal position

• Engine temperature

•Exterior temperature to determine viscosity of transmission fluid at low temperatures

• Steering wheel angular position to avoid shifting during a cornering maneuver

• Brake pedal position

• Input shafts speeds.

3. POWERTRAIN MODELING

This chapter consists of general structure of entire model (Section 3.1), powertrain components' models in detail and dynamic and kinematic relations of the components.

In engine model (Section 3.2), torque production and dynamic characteristics of engine will be discussed. In clutch model (Section 3.3), variable friction coefficient depends on slipping speed, engaged and slipping states and transition logic between them will be treated. In transmission model (Section 3.4), mechanical layout of the transmission, synchronizer model, later on, dynamic and kinematic relations will be explained. The chapter will be ended with vehicle dynamics and dynamic tyre and differential models and assumptions (Section 3.5, Section 3.6).

3.1 Structure of Entire Model

A powertrain model with dry dual clutch transmission is developed in this study.

5 Degrees of freedom (DoF) powertrain model (while both of clutches are slipping) is adopted. The model has 4 DoF while one of clutches is engaged (clutch input and output sides are rotating at the same speed). The model contains two spring-damper elements between clutch outputs and gearbox inputs due to clutch torsion springs and primiray shafts. Half shaft is also considered as a spring-damper element between differential and wheel as can be seen in Figure 3.1.

Damping coefficients are defined on differential and gearbox inputs in order to represent drag effect of oil especially on gears. Similarly, engine has also damping coefficient

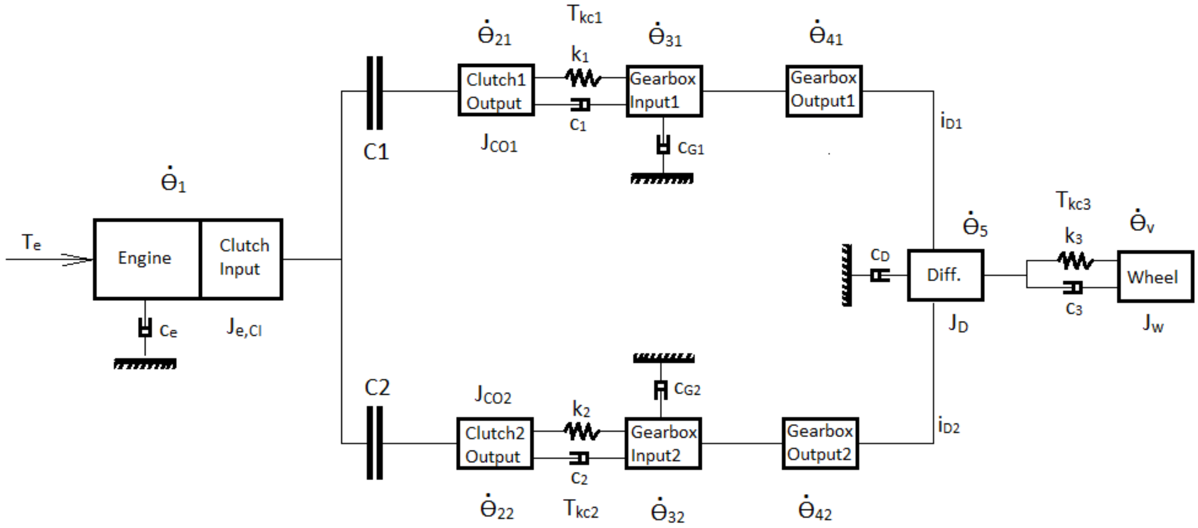

Figure 3.1 : Free body diagram of the powertrain.

Elements in the structure can be divided into two category as inertial elements (mass) and compliant elements (spring-damper, friction surfaces, tire slip etc.). Input and output variable of inertial elements are torque and speed respectively, whereas, compliant elements accept speed as input and generate torque as output variable. This modeling attitude provides consequent cause and effect relationship between input and output variables, and reduce algebraic equations (Goetz 2005).

Powertrain elements and flow of torque and speed variables through the elements is depicted in Figure 3.2.

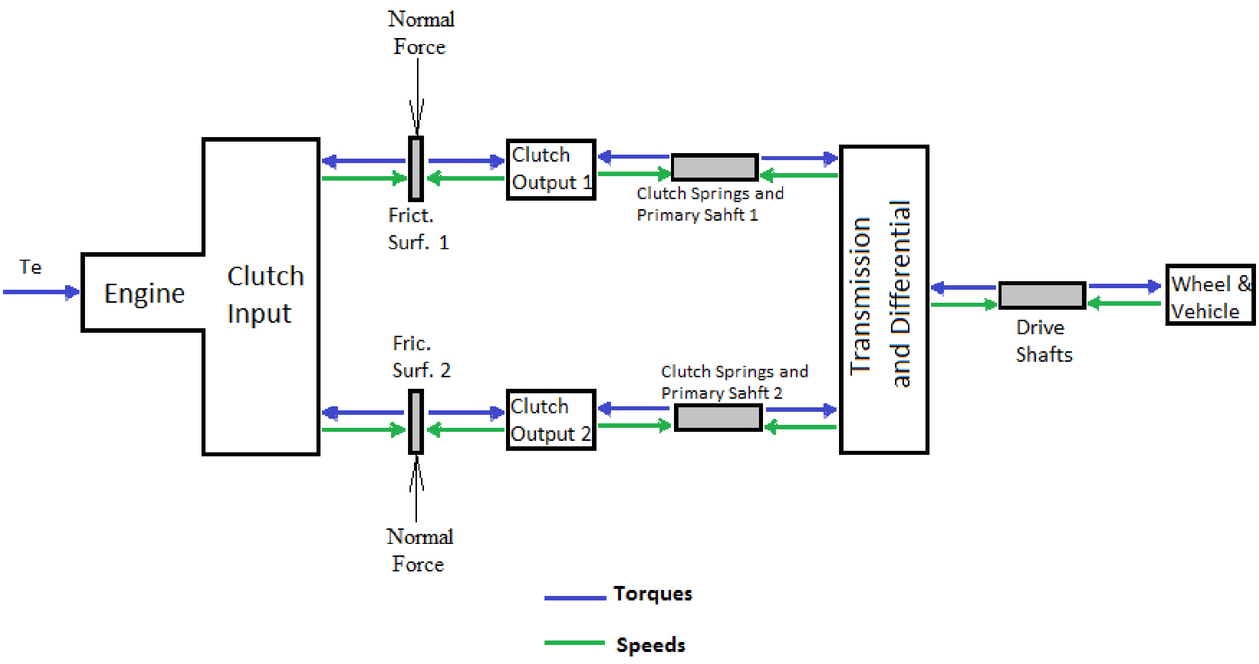

Figure 3.2 : Principle scheme of toque and speed flow throughout the powertrain.

In Figure 3.2, grey blocks represent compliant elements while other blocks represent inertial elements in the model.

3.2 Engine Model

In this study, mean value engine model is adopted in terms of torque production of engine. Namely, engine harmonic characteristic, due to piston by piston firing and rotational dynamics, is neglected. Engine harmonics do not have substantial effect on longitudinal dynamics of vehicle since harmonic frequencies are relatively high and spring-damper elements there exist.

Look-up table is used in order to represent engine torque production. Torque value is determined by the help of 1-D look-up table as function of engine speed from experimental data, and multiplied by acceleration pedal position.

Torque and power profiles derived from torque values are depicted in following graph (Figure 3.3).

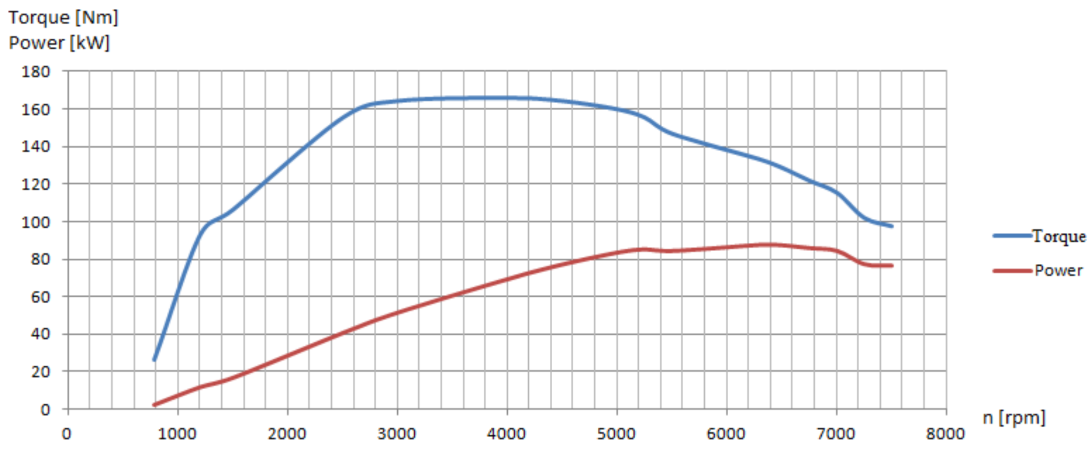

Figure 3.3 : Engine torque look-up table and power graph.

In order to derive dynamic equations of motion of engine, $\ddot{\theta}_1, \ddot{\theta}_{21}$ and $\ddot{\theta}_{22}$ are can be derived seperetaly according to two different states of clutces; "Engaged mode" and "Slipping mode". Dynamic equations of the other inertial elements can be considered independent from these modes due to elastic spring-damper elements located beforehand.

3.2.1 Slipping mode

In slipping mode, two case is possible: The first case; both clutches are slipping and transmitting torque. The second case; one of clutches is slipping and the other one is disengaged. In modeling, disengaged position is considered as slipping (clutch input and output speeds are different) but transmitting zero torque. It is also possible that both clutches are disengaged but in practice, it only occurs during neutral position. Two disengaged clutch during driving, means torque interruption which contradicts with the aim of dual clutch transmissions.

And the equations of motion of engine and clutch input side are as follows:

$$\left(J_{e,CI}\right)\ddot{\theta}_1 = T_e - \dot{\theta}_1 c_e - T_{C1} - T_{C2} \qquad \mathbf{(3.1)}$$

$$\ddot{\theta}_1 = \frac{T_e - \dot{\theta}_1 c_e - T_{C1} - T_{C2}}{J_{e,CI}} \qquad \mathbf{(3.2)}$$

Where, T_{C1} and T_{C2} are friction torques that transmitted via the clutches. Damping coefficient c_e is defined on the purpose of representing accessory loads.

Equations of motion of clutch output sides are:

$$J_{CO1}\,\ddot{\theta}_{21} = T_{C1} - T_{kc1} \qquad \mathbf{(3.3)}$$

$$\ddot{\theta}_{21} = \frac{T_{C1} - T_{kc1}}{J_{CO1}} \quad (3.4)$$

$$J_{CO2}\,\ddot{\theta}_{22} = T_{C2} - T_{kc2} \quad (3.5)$$

$$\ddot{\theta}_{22} = \frac{T_{C2} - T_{kc2}}{J_{CO2}} \quad (3.6)$$

Where, T_{kc1} and T_{kc2} are torque of spring-damper elements (clutch torsion springs) between clutches' output sides and gearboxes' input sides as shown in the Figure 3.1 above. And the equations of this elements is:

$$T_{kc1} = k_1(\theta_{21} - \theta_{31}) + c_1(\dot{\theta}_{21} - \dot{\theta}_{31}) \quad (3.7)$$

$$T_{kc2} = k_2(\theta_{22} - \theta_{32}) + c_2(\dot{\theta}_{22} - \dot{\theta}_{32}) \quad (3.8)$$

3.2.2 Engaged mode

Engine, cluth input and clutch output inertial elements have different equations of motion at the engaged state of clutches. The equations are as follows:

$$\left(J_{e,CI} + J_{CO_{eng}}\right)\ddot{\theta}_1 = T_e - \dot{\theta}_1 c_e - T_{C_{dis}} - T_{kc_{eng}} \quad (3.9)$$

$$\ddot{\theta}_1 = \frac{T_e - \dot{\theta}_1 c_e - T_{C_{dis}} - T_{kc_{eng}}}{J_{e,CI} + J_{CO_{dis}}} \quad (3.10)$$

Where, subscript 'eng' refers engaged clutch side and subscript 'dis' refers disengaged or slipping clutch side.

In the engaged state output side of the engaged clutch rotate coupled with clutch input side and the engine. Therefore, Newtonian equations of motion of clutch output sides are:

$$\ddot{\theta}_{2_{eng}} = \ddot{\theta}_1 \quad (3.11)$$

$$J_{CO_{dis}}\,\ddot{\theta}_{2_{dis}} = T_{C_{dis}} - T_{kc_{dis}} \quad (3.12)$$

$$\ddot{\theta}_{2_{dis}} = \frac{T_{C_{dis}} - T_{kc_{dis}}}{J_{CO_{dis}}} \quad (3.13)$$

3.3 Clutch Model and Friction

Elastic elements between clutch outputs and gearbox inputs represent torsional elasticity feature of primary shafts and clutch torsion springs. In fact, elasticity of primary shafts may be varied according to current gear, namely path of torque flow, due to different proportion of primary shaft that transmitting torque. And characteristic elasticity coefficient of clutch torsion springs may be considered at four different stage, according to angle of distorsion. But these characteristics are simplified and represented by one elasticity and one damping coefficient.

Clutch friction model can be divided into two modes as mentioned before. At the engaged mode, maximum torque that can be transmitted by clutch determined by static friction coefficient ($\boldsymbol{\mu}_{st}$) and the maximum turque at the engaged mode is:

$$\mathrm{T}_{\mathrm{C}_{\mathrm{eng}}\mathrm{max}} = (\mathrm{F}\ \mu_{\mathrm{st}}\ \mathrm{R}_{\mathrm{m}}\ \mathrm{Z}) \qquad \textbf{(3.14)}$$

Where, Z is number of friction surfaces, F is normal force applied on clutch surfaces and Rm is mean clutch radius:

$$\mathrm{R}_{\mathrm{m}} = \frac{2\left(\mathrm{R_o}^3 - \mathrm{R_i}^3\right)}{3\left(\mathrm{R_o}^2 - \mathrm{R_i}^2\right)} \qquad \textbf{(3.15)}$$

Where, Ro is outer radius and Ri is inner radius of friction surfaces in terms of meter.

Higher value of T_{Cmax} than actual torque transming through clutch T_C, is ensure remaining at engaged mode. As soon as clutch torque T_{Ci} surpass T_{Cimax}, clutch state change over to slipping mode.

To derive torque transmitting through engaged clutch, clutch input and output elements' torque balance equations, involving T_{Ceng} terms, must solved together.

$$\mathrm{J}_{\mathrm{e,CI}}\ \ddot{\theta}_1 = \mathrm{T_e} - \dot{\theta}_1\ \mathrm{c_e} - \mathrm{T}_{\mathrm{C}_{\mathrm{eng}}} - \mathrm{T}_{\mathrm{C}_{\mathrm{dis}}} \qquad \textbf{(3.16)}$$

$$\mathrm{J}_{\mathrm{CO}_{\mathrm{eng}}}\ \ddot{\theta}_{2_{\mathrm{eng}}} = \mathrm{T}_{\mathrm{C}_{\mathrm{eng}}} - \mathrm{T}_{\mathrm{kc}_{\mathrm{eng}}} \qquad \textbf{(3.17)}$$

At the engaged mode, these two inertial elements rotating coupled (same speed and acceleration).

$$\ddot{\theta}_{2_{\mathrm{eng}}} = \ddot{\theta}_1 \qquad \textbf{(3.18)}$$

Solving (3.16) and (3.17) together:

$$\left(J_{e,CI} + J_{CO_{eng}}\right) \ddot{\theta}_1 = T_e - \dot{\theta}_1\, c_e - T_{C_{dis}} - T_{kc_{eng}} \tag{3.19}$$

And entering the result of $\ddot{\theta}_1$ from (3.16) or (3.17) to the above equation (3.19):

$$\left(J_{e,CI} + J_{CO_{eng}}\right)\left(\frac{T_{C_{eng}} - T_{kc1}}{J_{CO_{eng}}}\right) = T_e - \dot{\theta}_1\, c_e - T_{C_{dis}} - T_{kc_{eng}} \tag{3.20}$$

If the equation is solved for $T_{C_{eng}}$:

$$T_{C_{eng}} = \frac{\left(T_e - \dot{\theta}_1\, c_e - T_{C_{dis}}\right) J_{CO_{eng}} + \left(T_{kc_{eng}}\right) J_{e,CI}}{J_{CO_{eng}} + J_{CI}} \tag{3.21}$$

As soon as clutch torque $T_{C_{eng}}$ surpass $T_{C_{max}}$, slipping mode is active. From that moment, transmitted torque through clutch is determined by dynamic friction coefficient ($\boldsymbol{\mu}_{dyn}$)

$$T_{C_{dis}} = \left(F\, \mu_{dyn}\, R_m\, Z\right) \operatorname{sign}\left(\dot{\theta}_1 - \dot{\theta}_{2_{dis}}\right) \tag{3.22}$$

The transition logic between engaged and slipping modes is:

$$\text{Engaged mode} \quad \rightarrow \quad \text{If}\left[\left|T_{C_{eng}}\right| > T_{C_{max}}\right] \quad \rightarrow \quad \text{Slipping mode} \tag{3.23}$$

$$\text{Slipping mode} \rightarrow \ \text{If}\left[\dot{\theta}_1 = \dot{\theta}_{2_{dis}} \text{and } \left(\left|T_{C_{eng}}\right| \le T_{C_{max}}\right)\right] \rightarrow \text{Engaged mode} \tag{3.24}$$

During slipping mode, clutch remains slipping as long as speed difference of clutch surfaces is higher than zero. As soon as the speed difference reaches zero, the simulation calculates $T_{C_{eng}}$, compares it with $T_{C_{max}}$ and determines that clutch will whether remain slipping or transit to engaged mode.

3.3.1 Dynamic friction coefficient

The simplest friction model is to define static friction coefficient and constant but lower dynamic friction coefficient (Coulomb friction). Drawbacks of this model are being not representative of reality and containing discontinuity in transition between engaged and slipping modes which causes simulation problems.

The friction coefficient profile may be investigated in three different region in order to obtain more realistic friction model. This model, adopted in this study, is depicted in the Figure 3.4:

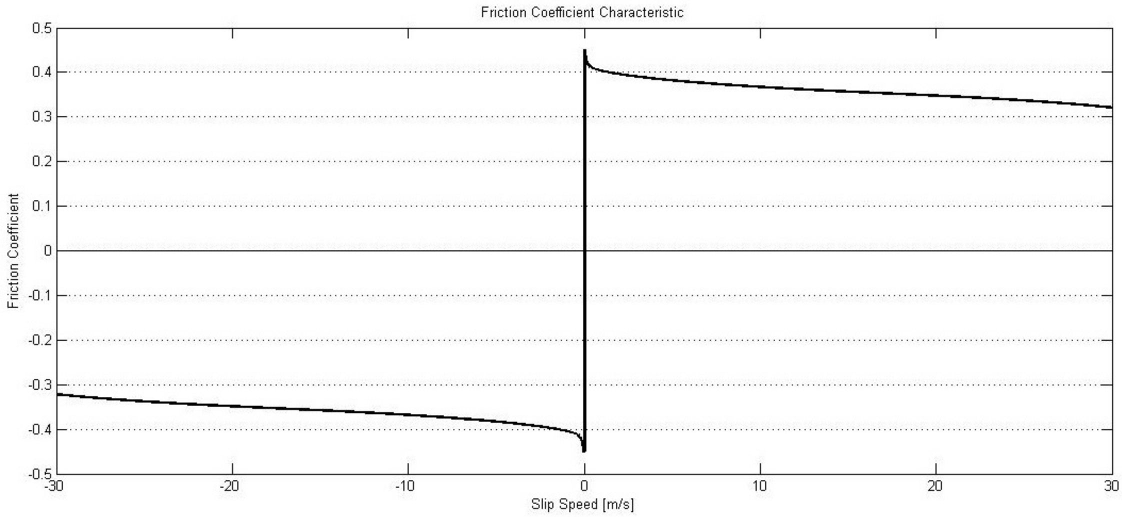

Figure 3.4 : Slip speed-friction coefficient characteristic curve.

The first region is static friction which occurs at engaged state same as mentioned above pharagraph. And the friction torque value at this state may lie between $T_{C_{max}}$ and $-T_{C_{max}}$ The second one is at the vicinity of zero slip speed, which is called as Stribeck frictions. This region, which also prevents discontinuity between static and dynamic friction, is active right after static friction threshold is surpassed. Stribeck frictions are shown in Figure 3.5:

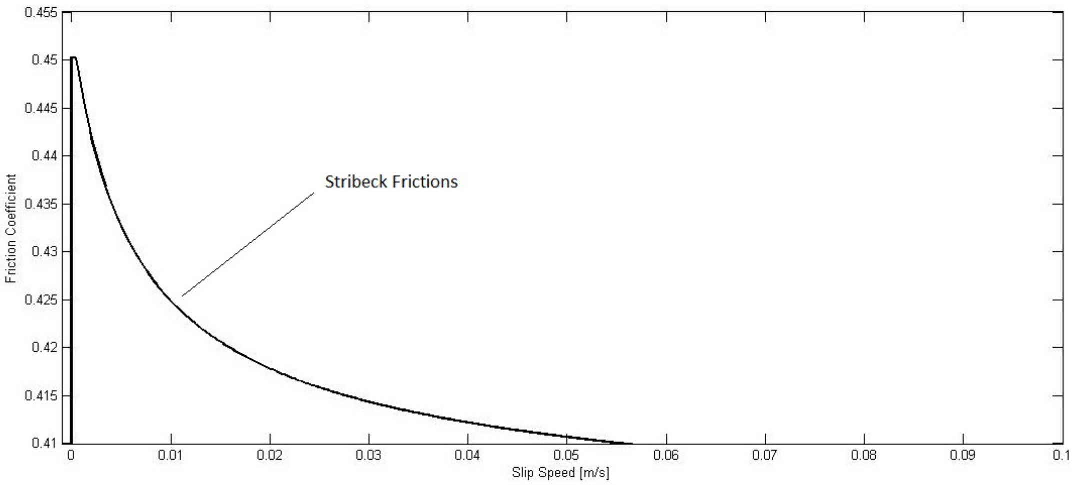

Figure 3.5 : Slip speed-Friction coefficient curve at stribeck friction region.

Stribeck frictions profile can be approached by the help of exponential equation:

$$\mu_{dyn1} = \mu_{coulomb} + \frac{(\mu_{st} - \mu_{coulomb})}{\ln(c\,.\,S + e)} \qquad \mathbf{(3.25)}$$

Where, S is slip speed in terms of (m/s) and $\mu_{coulomb}$ is the value that equation converges asymptotically while slip is going to infinity.

The third region is the rest of dynamic friction profile. For dry clutches, negative gradient friction coefficient profile with slip speed, is used in this study, as can be seen in Figure 3.4. This profile can be fitted by the help of a three degree polynomial equation:

$$\mu_{dyn2} = A.S + B.S^2 + C.S^3 \qquad (\mathbf{3.26})$$

Sum of these two equation can be used as dynamic friction model:

$$\mu_{dyn} = \mu_{coulomb} + \frac{(\mu_{st} - \mu_{coulomb})}{\ln(c.S + e)} + A.s + B.S^2 + C.S^3 \qquad (\mathbf{3.27})$$

Where, c, A, B and C are coefficients. (Goetz 2005).

$$S = \left(\dot{\theta}_1 - \dot{\theta}_{2_{dis}}\right) R_m \qquad (\mathbf{3.28})$$

3.4 Transmission Model

The mechanical layout of DCT, which is adopted in this study, is depicted in Figure 3.6 A 6 speed dry clutch DCT design is used. 1st, 3rd and 5th gearwheels are meshed with gearwheels of primary shaft 1 (solid shaft, P1). 2nd, 4th, 6th and reverse gearwheels are meshed with gearwheels of primary shaft 2 (hollow shaft, P2). The torque flow is transmitted to final drive by means of synchronizers (s_{R4}, s_3, s_{26}, s_{15}) and gearwheels of secondary shafts (S1 nad S2).

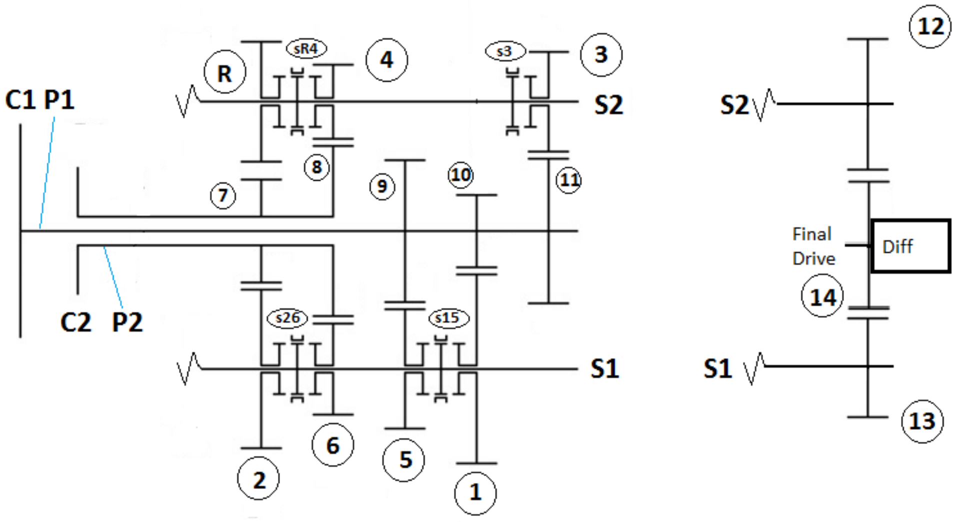

Figure 3.6 : The mechanical layout of the DCT model.

In this design, the torque flows from primary shaft 1 and 2 may be transmitted via different or the same secondary shafts. For instance, during shifting process between 3rd and 4th gears (both clutches are slipping), torque flows from both clutch 1 (C1) and clutch 2 (C2) is transmitted to secondary shaft 2 and final drive gearwheels by means of synchronizers s3 and sR4. Final drive unit consists of end gears of secondary shafts (12 and 13) and gear 14, which is ring gear of differential at the same time. These unit has also two different final gear ratio for each secondary shaft.

Following inertial elements of gearbox have independent equations of motion from engaged or disengaged modes of clutches. And the kinematic equations of gearbox input and output sides are:

$$\ddot{\theta}_{31} = i_{cur1}\, i_{D1}\, \ddot{\theta}_5 \qquad (\mathbf{3.29})$$

$$\ddot{\theta}_{32} = i_{cur2}\, i_{D2}\, \ddot{\theta}_5 \qquad (\mathbf{3.30})$$

$$\ddot{\theta}_{41} = i_{D1}\, \ddot{\theta}_5 \qquad (\mathbf{3.31})$$

$$\ddot{\theta}_{42} = i_{D2}\, \ddot{\theta}_5 \qquad (\mathbf{3.32})$$

Where, $i_{cur1,2}$ are ratios of currently selected and preselected gears on secondary shaft 1 and/or secondary shaft 2 (S1 and S2). And $i_{D1,2}$ are ratios of secondary shaft 1 and 2 (S1 and S2) final drive gears.

$$i_1 = \frac{z_1}{z_{10}}\ , \qquad i_3 = \frac{z_3}{z_{11}}\ , \qquad i_5 = \frac{z_5}{z_9} \qquad (\mathbf{3.33})$$

$$i_2 = \frac{z_2}{z_7}\ , \qquad i_4 = \frac{z_4}{z_8}\ , \qquad i_6 = \frac{z_6}{z_8} \qquad (\mathbf{3.34})$$

$$i_{D1} = \frac{z_{14}}{z_{13}}\ , \qquad i_{D2} = \frac{z_{14}}{z_{12}} \qquad (\mathbf{3.35})$$

Where, z is gear teeth number.

The dynamic equation of differential can be derived by reducing gearbox inertias into differential.

$$\left(J_{D_{eq}}\right)\, \ddot{\theta}_5 = T_{D_{eq}} - T_{kc3} - \dot{\theta}_5\, c_D \qquad (\mathbf{3.36})$$

$$\ddot{\theta}_5 = \frac{T_{D_{eq1}} + T_{D_{eq2}} - T_{kc3} - \dot{\theta}_5\, c_D}{J_{D_{eq}}} \qquad (\mathbf{3.37})$$

Where, $J_{D_{eq}}$ is equivalent moment of inertia of primary shafts, gears, secondary shafts and synchronizers on the differential. $T_{D_{eq1,2}}$ are equivalent torques due to spring damper elements (T_{kc1} and T_{kc2}) and damping coefficients (c_{G1} and c_{G2}) at the differential. Shafts, gears and synchronizers are depicted in mechanical layout in the Figure 3.6 above.

T_{kc3} is torque of spring-damper element (sum of two half shafts) between differential and wheels, and:

$$T_{D_{eq1}} = \left(k_1(\Theta_{21} - \Theta_{31}) + c_1\left(\dot{\Theta}_{21} - \dot{\Theta}_{31}\right) - \dot{\Theta}_{31}\, c_{G1}\right) i_{cur1}\, i_{D1} \qquad (\mathbf{3.38})$$

$$T_{D_{eq2}} = \left(k_2(\Theta_{22} - \Theta_{32}) + c_2\left(\dot{\Theta}_{22} - \dot{\Theta}_{32}\right) - \dot{\Theta}_{32}\, c_{G2}\right) i_{cur2}\, i_{D2} \qquad (\mathbf{3.39})$$

In order to obtain equivalent moments of inertia at the differential, 1) Secondary shafts (S1 and S2) and synchronizers, 2) Primary shafts (P1 and P2) and all gears meshed with them are considered separately. Namely, first of all equivalent moments of inertia of gears on primary shafts ($J_{P1_{eq}}$ and $J_{P2_{eq}}$) may be derived as follows:

$$J_{P1_{eq}} = J_{P1} + J_9 + J_{10} + J_{11} + \frac{J_1}{{i_1}^2} + \frac{J_3}{{i_3}^2} + \frac{J_5}{{i_5}^2} \qquad (\mathbf{3.40})$$

$$J_{P2_{eq}} = J_{P2} + J_7 + J_8 + \frac{J_2}{{i_2}^2} + \frac{J_4}{{i_4}^2} + \frac{J_6}{{i_6}^2} + \frac{J_R}{{i_R}^2} \qquad (\mathbf{3.41})$$

Then, equivalent moments of inertia at P1 and P2 ($J_{P1_{eq}}$ and $J_{P2_{eq}}$) and that of S1, S2, synchronizers and final gears must be reduced to the differential.

$$J_{GO1} = J_{S1} + J_{s2-6} + J_{s1-5} + J_{13} \qquad (\mathbf{3.42})$$

$$J_{GO2} = J_{S2} + J_{sR-4} + J_{s3} + J_{12} \qquad (\mathbf{3.43})$$

Finally, equivalent moments of inertia of all transmission inertial elements at the differential is:

$$J_{D_{eq}} = J_D + J_{GO1}\, {i_{D1}}^2 + J_{GO2}\, {i_{D2}}^2 + J_{P1_{eq}}\, {i_{cur1}}^2\, {i_{D1}}^2 + J_{P2_{eq}}\, {i_{cur2}}^2\, {i_{D2}}^2 \qquad (\mathbf{3.44})$$

As can be seen from the above equation (3.44), equivalent moments of inertia at the differential depends on current selected and preselected gears.

For instance, when actual gear is 1 and 2nd gear is preselected, equivalent moments of inertia of transmission elements at the differential is 3.0299 kgm^2. While that of 6th actual gear and 5th preselected gear is 0.4119 kgm^2.

3.5 Differential Wheels and Tyres

In this study, longitudinal dynamics of vehicle taken into account solely. Lateral and vertical dynamics are neglected. It is also assumed that there exists no inequal torque distribution on right and left halfshafts. Consequently, differential can be considered as only a inertial mass on the assumption that side gears of differential rotate at the same speed.

In a similar manner, two driven wheels are always rotate at the same speed on the assumption that same resistive forces and road conditions acting on both of wheels. Therefore, wheels can be considered as lumped together.

Consequently, equivalent torsional elasticity and damping are used for lumped halfshafts.

Equations of motion of wheel is as follows:

$$\ddot{\theta}_w J_w = k_3(\theta_5 - \theta_w) + c_3(\dot{\theta}_5 - \dot{\theta}_w) - T_{Resistive} \quad (\mathbf{3.45})$$

$$\ddot{\theta}_w = \frac{k_3(\theta_5 - \theta_w) + c_3(\dot{\theta}_5 - \dot{\theta}_w) - T_{Resistive}}{J_w} \quad (\mathbf{3.46})$$

In this study, elasticity and slipping characteristic of tyres is neglected in order to simplify the model. Namely, there exists no compliant element between wheel and road. Consequtively, speed and acceleration of vehicle directly depend on wheel's rotational speed.

$$V_v = \dot{\theta}_w \, r_{tyre} \quad (\mathbf{3.47})$$

$$a_v = \ddot{\theta}_w \, r_{tyre} \quad (\mathbf{3.48})$$

3.6 Vehicle Dynamics

$$T_{Resistive} = (F_R + F_A + F_{Acc} + F_{Grad}) \, r_{tyre} \quad (\mathbf{3.49})$$

Where, F_R is rolling resistance, F_A is aerodynamic resistance, F_{Acc} is acceleration resistance, F_{Grad} is resistance of road gradient and rtyre is radius of wheels. Tractive and resistive forces acting on vehicle are depicted in Figure 3.7.

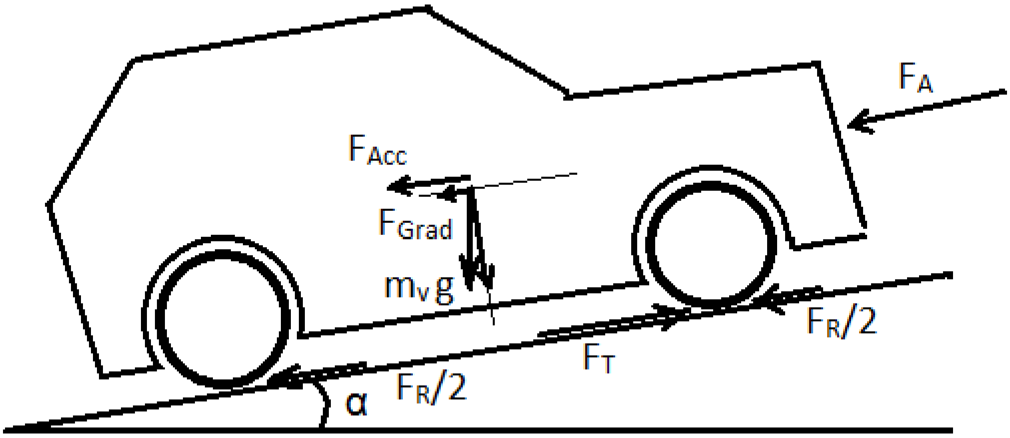

Figure 3.7 : Resistive forces acting on the vehicle.

The resistive forces are:

$$F_{Grad} = \sin(\alpha)\ m_v\, g \tag{3.50}$$

$$F_A = \frac{1}{2}\, V_v{}^2\, C_D\, A\ \rho \tag{3.51}$$

$$F_R = \cos(\alpha)\ m_v\, g\, f \tag{3.52}$$

Where, m_v is vehicle mass, g is gravitational acceleration, C_D is aerodynamic drag coefficient, A is frontal area of the vehicle, ρ is air density and f is rolling resistance coefficient.

$$F_{Acc} = a_v\, M_v \tag{3.53}$$

M_v is total vehicle mass with reduced non-driven rotational parts to wheel, and:

$$M_v = m_v + \frac{J_{non-driv}}{r_{tyre}{}^2} \tag{3.54}$$

4. POWERTRAIN CONTROL

In the beginning of this chapter, gear shift schedule and preselection logic will be explained. In the following section, clutch control during shifting process will be discussed.

4.1 Shift Schedule

In this study, the moments, that upshift or downshift shifting process begins, are determined according to vehicle speed and accelerator pedal position. Namely, for any current gear position, there exist vehicle speed thresholds of upshift or downshift depending on accelerator pedal position. For high accelerator pedal positions, shifts are initiated at the engine speed that produces maximum power on the purpose of maximum overall acceleration. And for low accelerator pedal positions, shifts take place at low engine speeds in order to provide low fuel consumption.

In the following graph (Figure 4.1) of engine speed according to vehicle speed, shift speeds are shown in cases of high APP and low APP.

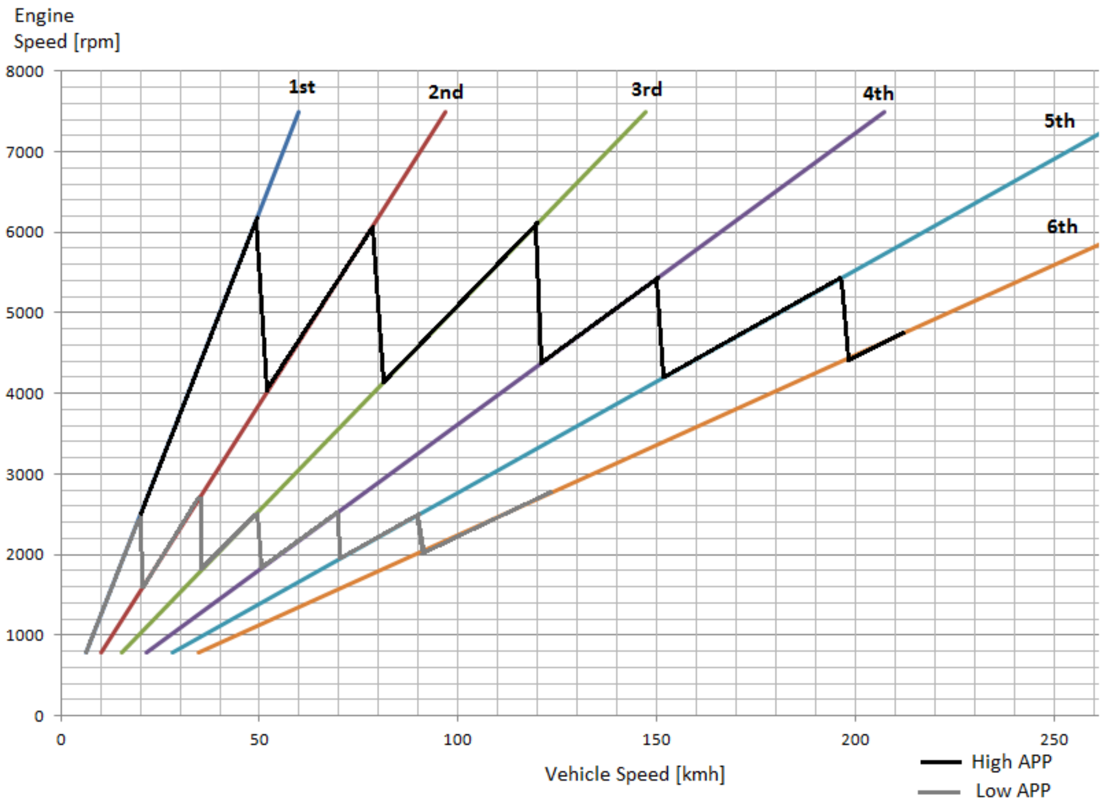

Figure 4.1 : Engine speed profiles accelerating vehicle with low APP and high APP.

The simulation compares actual vehicle speed with this threshold speeds for current accelerator pedal position at each instant time. Then it decides whether clutch operation will be initiated for shifting process or the current gear position will remain.

Example of upshift or downshift thresholds of 3rd gear is depicted in Figure 4.2:

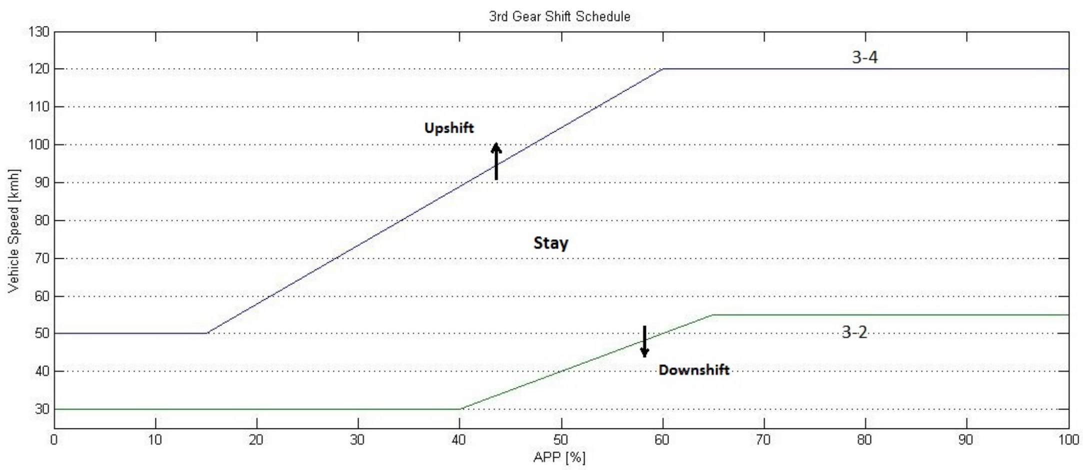

Figure 4.2 : Shift thresholds of 3rd gear.

The logic decides to stay at 3rd gear, if vehicle speed between 3-4 and 3-2 thresholds for instant APP and to initiate shifting process if speed is higher than 3-4 or lower than 3-2 thresholds. But, 3-4 upshift threshold and 4-3 downshift threshold are not coincident. There exists hysteresis area between thresholds in order to avoid repeated and frequent gear shifts due to speed changing during or right after shifting processes.

Hysteresis area between 1-2 upshift and 2-1 downshift thresholds is depicted in Figure 4.3:

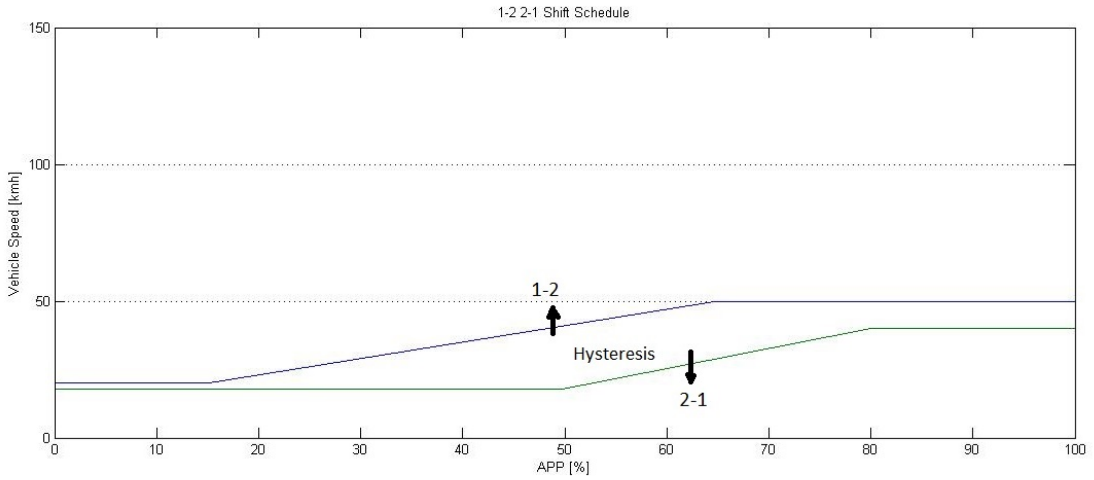

Figure 4.3 : Hysteresis area between 1-2 upshift and 2-1 downshift thresholds.

The entire shift schedule is shown in Figure 4.4:

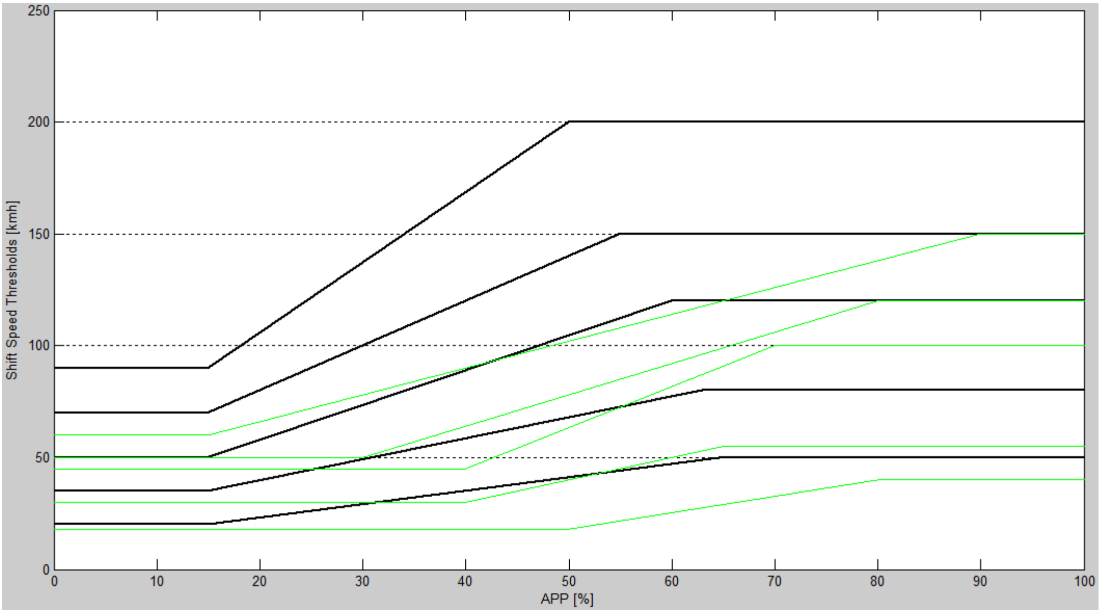

Figure 4.4 : Shift schedule of the automatic transmission.

During shifting process, the gear position is denoted by a value between actual gear and target gear for simulation. As soon as the clutch operation is finished, the target gear is active.

Multiple shifts are not considered in this study.

4.2 Gear Pre-Selection

Main advantage of dual clutch transmissions is shifting capabability without torque interruption in addition to its high efficiency. It is achieved by the help of the chance of pre-selecting target gear at any time and simultaneous clutch operation of actual and target gears during shifting process.

As mentioned, gearwheels of disengaged clutch (torque free half of transmission) can be pre-selected at any time. The pre-selection strategy, used in this study, is to keep next lower gear pre-selected for any current gear, and if target gear is higher gear, the pre-selection takes place when upshift is decided. This strategy aimed quick response for downshifts, especially in case of hard braking or high torque demand with high accelerator pedal position rate of change. It means, firstly pre-selection of higher gear must be implemented before an upshift and pre-selection of lower gear must be realized after a downshift completed to keep lower gear ready. Pre-selection and clutch operation schedule for any gear position are explained in the following Table4.1.

Table 4.1 : Synchronizer and clutch operation schedule for each gear and shift process.

UPSHIFTS			DOWNSHIFTS		
Gear	Selected synch. on secondary shaft 1 & 2	Clutch and Synchronizer Operation	Gear	Selected synch. on secondary shaft 1 & 2	Clutch and Synchronizer Operation
G=1	s1=1 s2=2	– –	G=6	s1=5 s2=6	– –
G=1.6	s1=1 s2=2	s=∅ C=C1→C2	G=5.4	s1=5 s2=6	C=C2→C1 –
G=2	s1=1 s2=2	– –	G=5	s1=5 s2=4	s=6→4 –
G=2.6	s1=3 s2=2	s1=1→3 C=C2→C1	G=4.4	s1=5 s2=4	C=C1→C2 –
G=3	s1=3 s2=2	– –	G=4	s1=3 s2=4	s=5→3 –
G=3.6	s1=3 s2=4	s2=2→4 C=C1→C2	G=3.4	s1=3 s2=4	C=C2→C1 –
G=4	s1=3 s2=4	– –	G=3	s1=3 s2=2	s=4→2 –
G=4.6	s1=5 s2=4	s1=3→5 C=C2→C1	G=2.4	s1=3 s2=2	C=C1→C2 –
G=5	s1=5 s2=4	– –	G=2	s1=1 s2=2	s=3→1 –
G=5.6	s1=5 s2=6	s2=4→6 C=C1→C2	G=1.4	s1=1 s2=2	C=C2→C1 –
G=6	s1=5 s2=6	– –	G=1	s1=1 s2=2	s=∅ –

4.3 Launch Control

In this study, engine manipulation strategy is not considered. However, clutch normal force is controlled in closed loop based on engine speed and acceleration during launch process.

At the beginning of the launch process, engine speed increases with a constant acceleration by the help of clutch actuation. Then engine speed is kept at a constant value due to clutch normal force, namely friction torque increases. When engine and P1 speeds are close, clutch normal force is reduced again to ensure smooth engaging. Figure 4.5 shows engine and primary shaft 1 speed profiles at the launch process

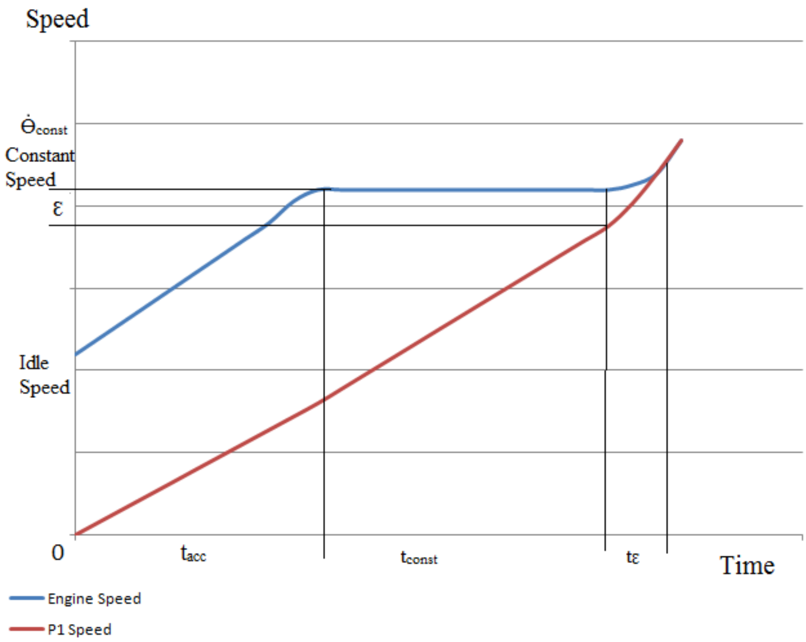

Figure 4.5 : Expected engine and primary shaft 1 speed profiles based on control strategy.

The launching logic is as follows:

$$\text{IF } \left[[\dot{\theta}_1 < \dot{\theta}_{const}] \ \text{ OR } \ [S_{C1} \leq Ɛ] \right] \rightarrow \ddot{\theta}_1 = a \qquad (\mathbf{4.1})$$

$$\text{ELSE} \rightarrow \ddot{\theta}_1 = 0 \qquad (\mathbf{4.2})$$

Where, S_{C1} is clutch 1 surfaces slip speed, $\dot{\theta}_{const}$ is constant engine speed which set by the help of fuzzy logic, Ɛ is clutch slip speed threshold at which tconst region will be ended just before engaging moment, a is constant engine acceleration value which is a positive valance.

Increasing engine speed with restricted acceleration provides low speed difference between clutch surfaces. It means low friction work and dissipation during launch process. Constant speed value of engine is determined by fuzzy logic according to APP. For instance, high constant engine speed is set, in case of APP between %70-100 in order to obtain high torque during launching. Clutch normal force decrease, consequtively engine speed increase, provides smoother engaging with low jerk intensity.

In some case, constant engine speed phase (t_{const}) may be bypassed.

4.4 Clutch Control

In this section, clutch actuation control strategies for power-on and power-off shifts will be explained in two parts. Power-on and power-off refer cases that vehicle is driven by engine and engine is driven by vehicle respectively.

Electro-mechanical actuator, which is driving diaphram springs of clutch pressure plates, is not considered in this study. Clutch surfaces normal force is represented as linear increment with actuation.

At the beginning of power-on shifts, engine speed surpasses offgoing clutch output speed when clutch slip starts as offgoing clutch is releasing. In contrast at the beginning of power-off shifts, engine speed drops below offgoing clutch output speed when clutch slip starts as offgoing clutch is releasing.

4.4.1 Power-on shift control

Dual clutch transmissions provide shifting without torque interruption by the help of separate control of both clutches' normal force at the same time. However, simultaneous operation of clutches have significant effect on torque variation, consecutively, on vehicle jerk intensity. Poor clutch control may cause high jerk intensity, even torque interruption.

During an upshift process, in case of early application of on-coming clutch normal force increase, off-going clutch speed may drop below that of engine, before it is entirely disangaged. It causes negative clutch torque on off-going clutch. In this study, during power-on shifts, the on-coming clutch normal force increase initiates whereafter positive off-going clutch slip occurs (Goetz 2005). It guarantees off-going clutch to be entirely disengaged by its slip speed drops below zero.

Moreover, excessive on-coming clutch normal force increase during inertia phase of power-on downshift or upshift may cause high torque hole or torque hump respectively. On-coming clutch normal force must be restricted at a proper value in order to avoid this effect. Prospective torque and transmission speed profiles are depicted in Figure 4.6:

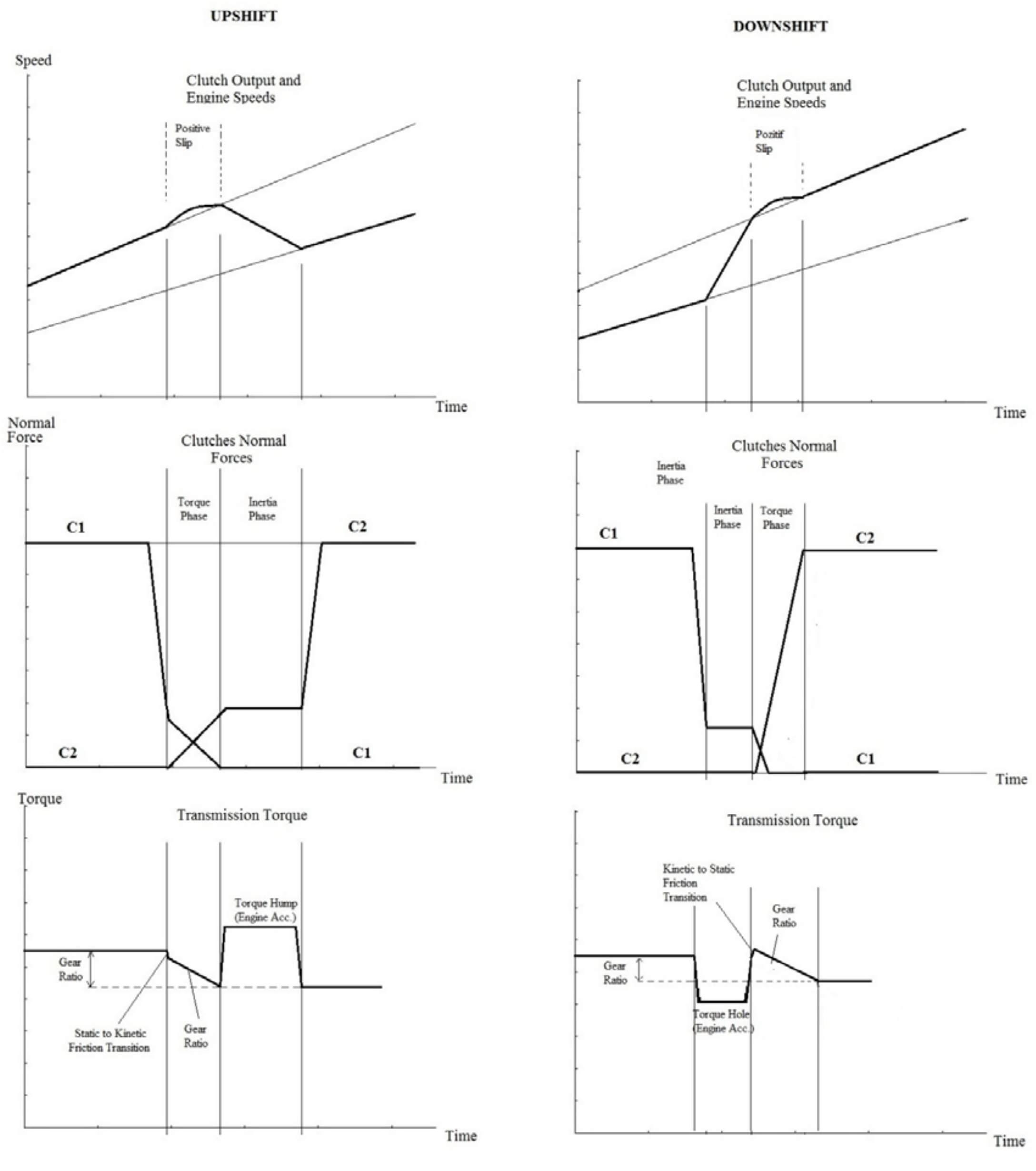

Figure 4.6 : Principle clutch control logic of power-on shifts.

At the power-on downshift process, firstly, engine speed is synchronized with on-coming clutch output speed (inertia phase), then simultaneous clutch actuation is executed. Namely, torque phase and inertia phase are translocated during downshift process. And the torque hump at upshift becomes torque hole due to positive engine acceleration.

4.4.2 Power-off shift control

Power-off shift control is less important than that of power-on shifts due to there exists no torque demand. During torque phase of power-off upshift clutch slip control is not used.

Expected engine and primary 1 and 2 shaft speed and clutch normal force profiles during power-off upshift an downshift profiles are as follows:

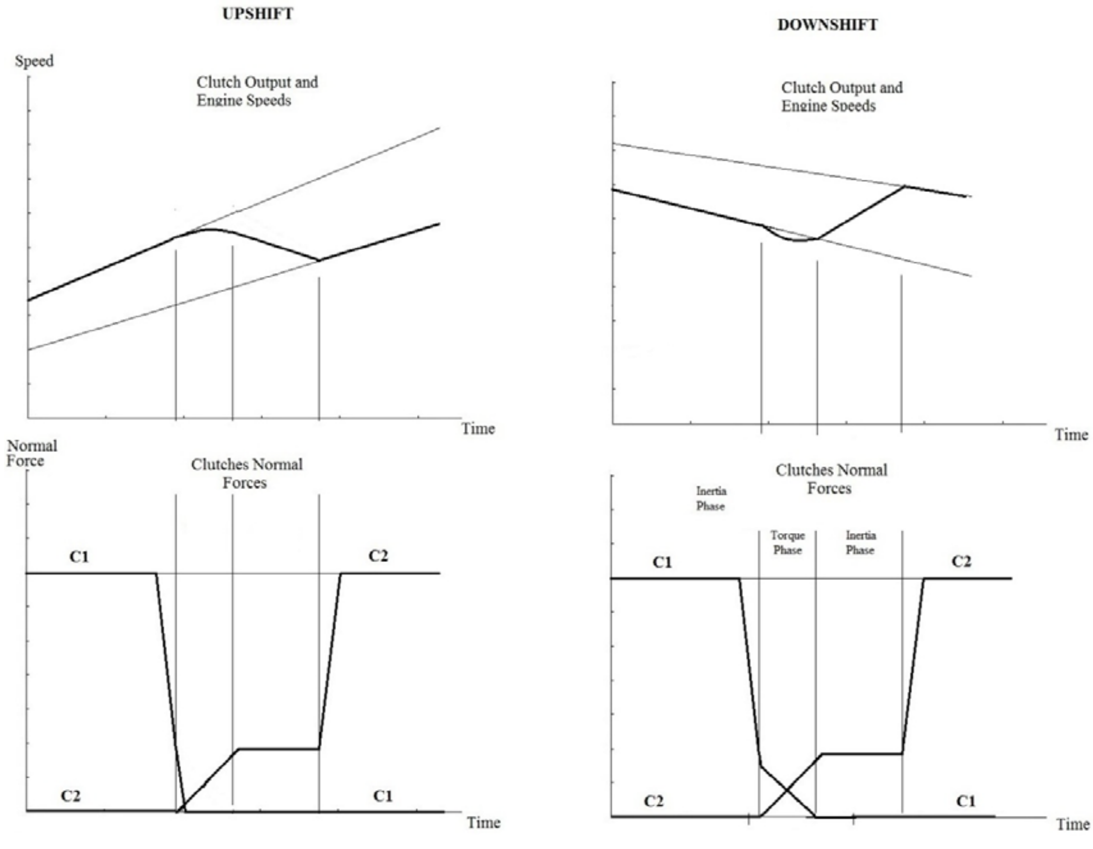

Figure 4.7 : Principle clutch control logic of power-off shifts.

Similar control strategies with power-on shifts are used for power-off downshift process.

4.5 Synchronizer Control

Synchronizer control is far less critical than that of clutch normal force and engine since synchronizer actuation realized on torque free half of the transmission. Inertial effect of disengaged clutch output, primary shaft and gearwheels is acting during synchronization.

In this study, synchronizer actuation is represented as switches to transmit torque free half gear ratios and equivalent inertias to next gear's values. However, the change of gear ratio is transformed to ramp function in order to represent synchronization time. Similarly, the change of equivalent inertias is transformed to ramp function on the purpose of avoiding discontinuities.

The change rate of gear ratios is chosen considering appropriate synchronization duration from literature.

5. SIMULATION RESULTS AND CONCLUSIONS

In this chapter, three different cases in terms of road gradient and accelerator pedal position (APP) will be defined and then simulation results of the cases will be discussed. The first case consists of launch and acceleration with high APP up to 5th gear. The second one contains various conditions including launch and acceleration with very low APP and negative road gradient (power-off upshifts), rapid APP increment (power-on downshift), acceleration with high APP and positive road gradient (power-on upshift), then sequent upshifts caused by rapid deceleration of APP. The last case is acceleration by low APP and negative gradient again, afterwards vehicle rapid coasting with zero APP and positive gradient (power-off downshifts). These cases are depicted in Figure 5.1.

Afterwards, the cases will be investigated in detail such as engine and primary shafts speed profiles, acceleration characteristics and clutch operations during launch and shifting processes seperately.

Aditionally, during shifting process, different clutch slip speed control strategy is used in order to reduce harshness at the vicinity of clutch engagement. Effects of the latter strategy on vehicle acceleration fluctuations is discussed in the first case.

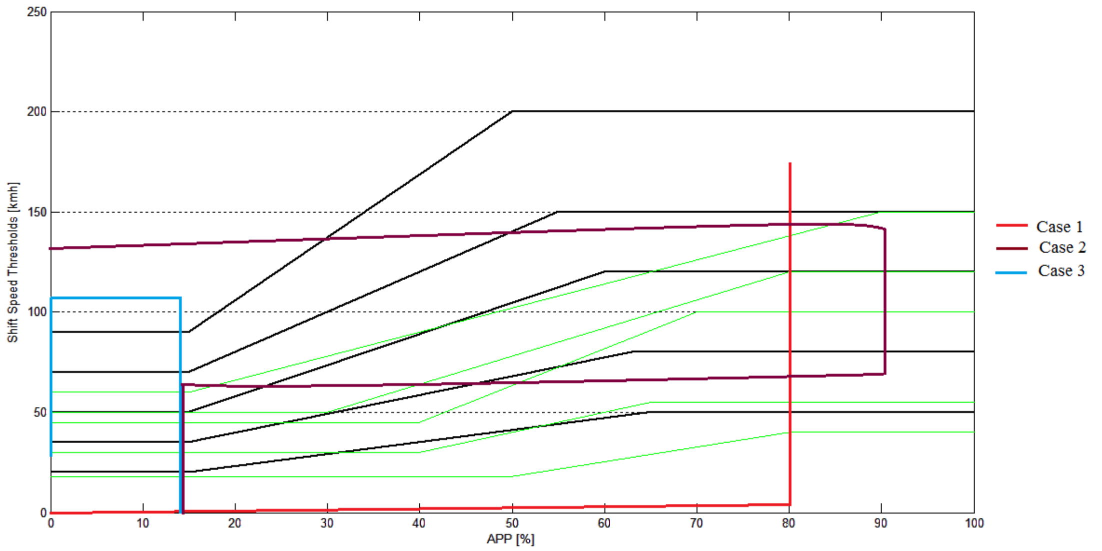

Figure 5.1 : Case studies adopted to examine the model.

5.1 Case 1

In this case, the vehicle is accelerated during 40 seconds by the APP increasing up to %80 with high rate of change. In the following figures (Figure 5.2), engine and primary shafts speeds, gear positions and clutch normal forces and vehicle speed and acceleration are shown.

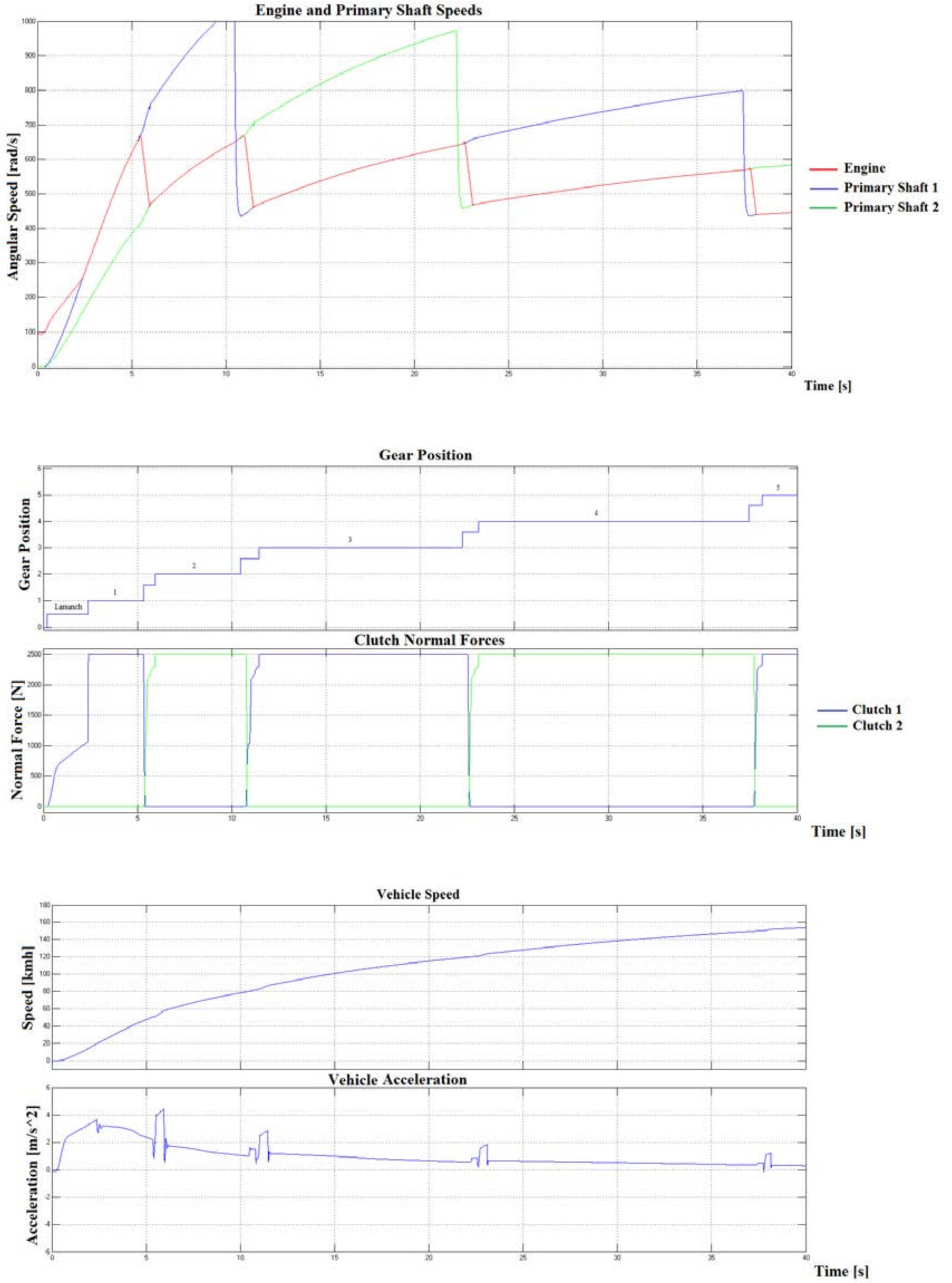

Figure 5.2 : Overall simulation result profiles of Case 1.

As can be shown in Figure 5.2 the vehicle speed surpassed 100 kmh in 15 seconds at the position of 3rd gear with %80 APP. According to gearshift schedule, upshifts occur at higher engine speeds in order to represent driver intention.

The engine and primary shafts speeds, namely the clutch input and outputs speeds are shown in Figure 5.2. As mentioned before, synchronizer operations are realized before that of the clutches for upshifts in order to keep lower gear ready. Simultaneous clutch normal force control of the same cycle also can be seen in Figure.. 5.2.

Later on in this section, clutch normal force control during gear shifting and launch, synchronizer changes and engine and primary shaft speed profiles of the same case will be treated in detail. Clutch 1 normal force control, engine and primary shaft speed profiles and vehicle acceleration during launching process are focused in Figure 5.3:

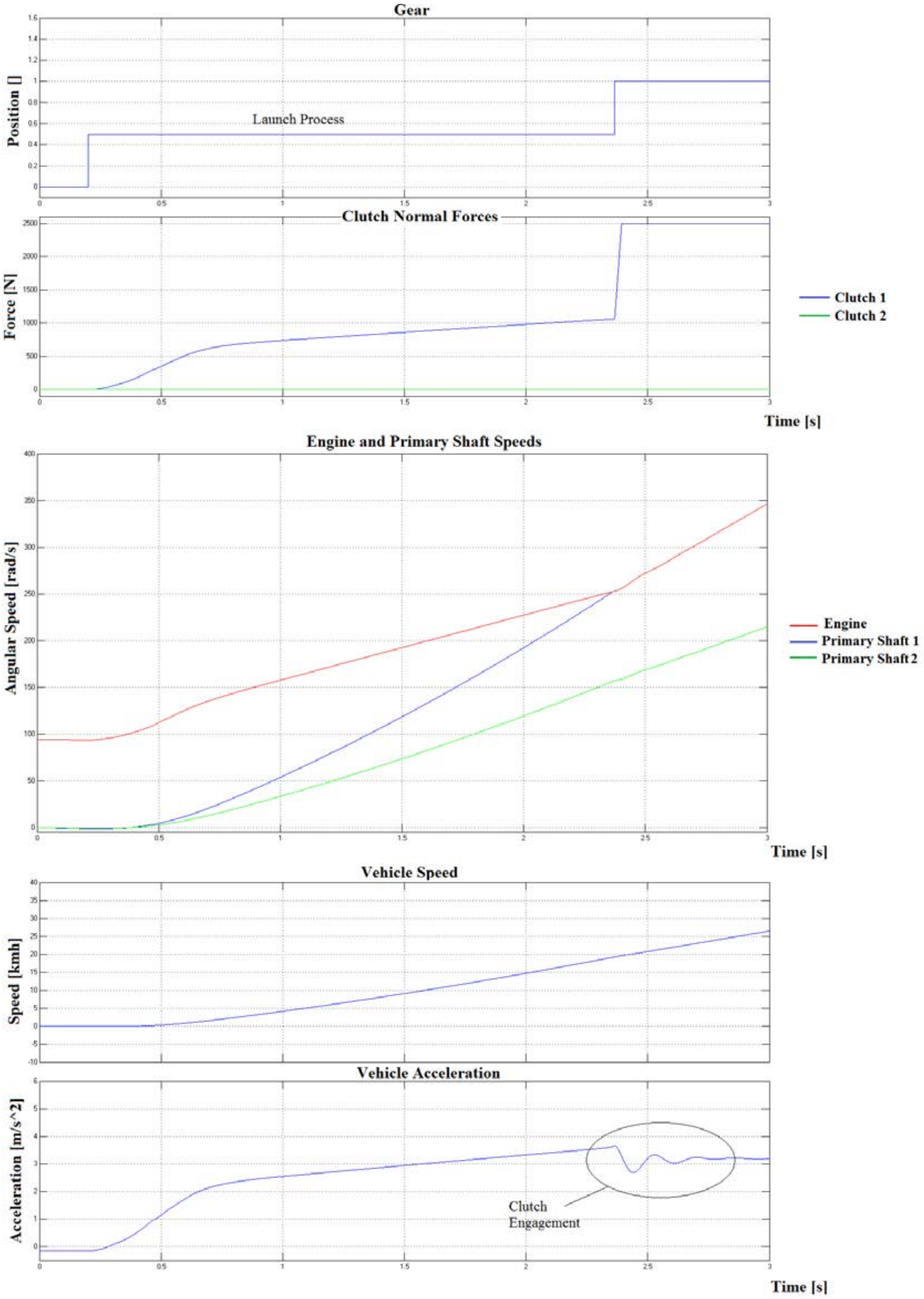

Figure 5.3 : Simulation results of launch process from Figure 5.2.

As can be seen in 'Clutch Normal Forces' graph, clutch 1 is controlled to provide constant engine acceleration during launching. This strategy reduces fluctuations at the clutch engagement moment while making use of high engine torque at higher speeds. Then the clutch normal force is increased to its engagement value after the engagement moment, which is 2500 N. Vehicle acceleration fluctuations produced by clutch engagement can be seen in the above figure as expected.

In the following figure (Figure 5.4), clutch normal force control, engine and primary shaft speed profiles and vehicle acceleration during 1st to 2nd gear upshift of the first case are shown. 1-2 upshift process is chosen to analyse due to its high primary shafts and clutch input-output speed difference.

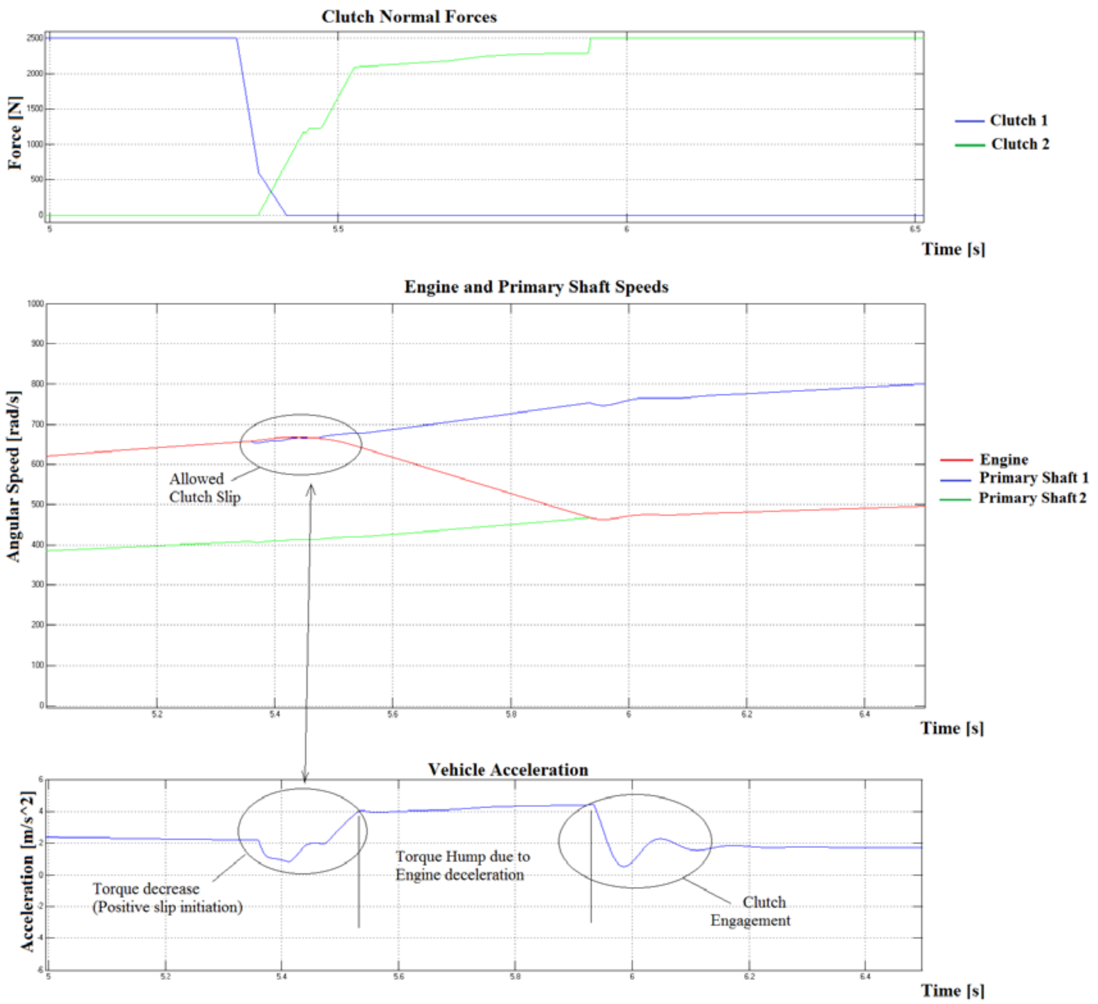

Figure 5.4 : Simulation results of 1-2 power-on upshift process from Figure 5.2.

In the following figure (Figure 5.5), simulation and experimental results are shown and compared from different study (Liu, Qin, Jiang, Zhang 2014) with similar shifting strategies for 1-2 upshift.

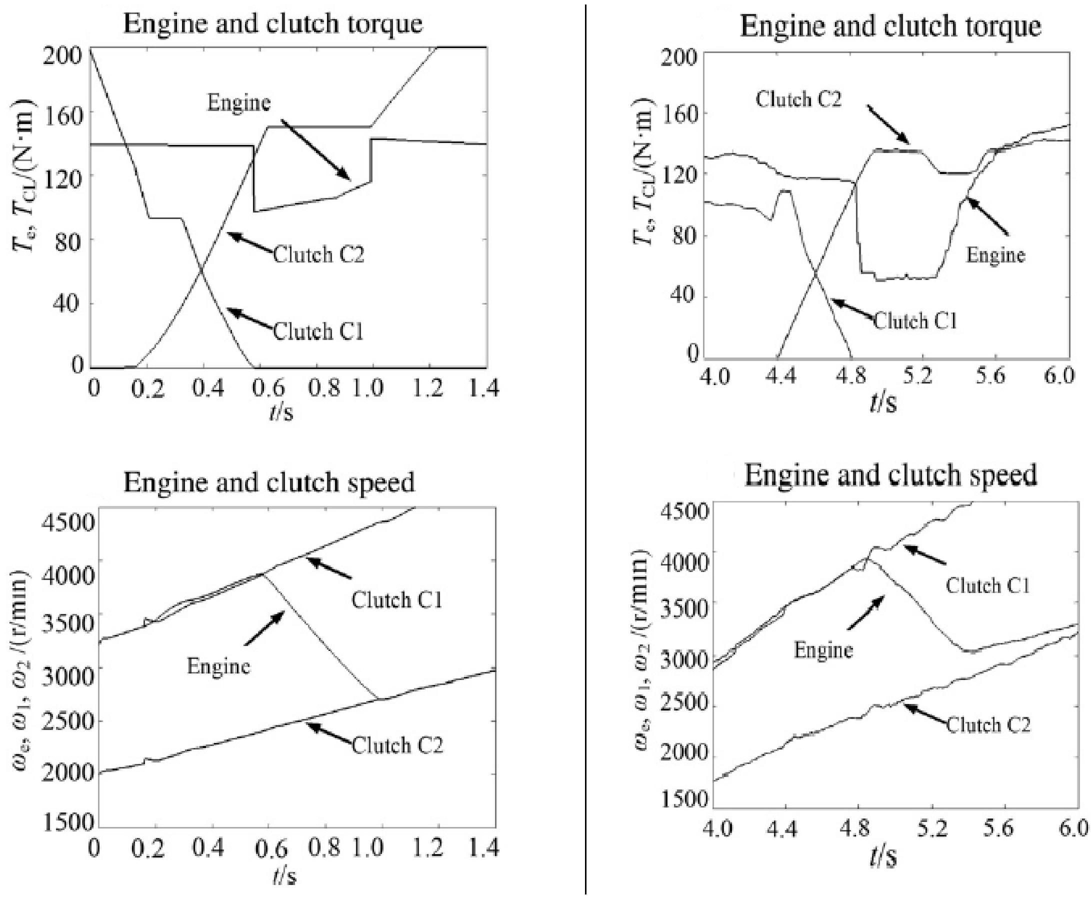

Figure 5.5 : Simulation and experimental results of 1-2 upshift process from different study (Liu, Qin, Jiang, Zhang 2014).

Engine and primary shaft speed and clutch actuation profiles, shown in Figure 5.5, are similar with that of this study (Figure 5.4). However, unlike (Liu, Qin, Jiang, Zhang 2014), engine manipulation strategies are not used in this thesis. Shift times of (Liu, Qin, Jiang, Zhang 2014) and that of this thesis are also close, which are about 0.8 seconds and 0.6 seconds respectively.

As can be seen in Figure 5.4, the vibrations at the engagement moment are relatively high. As mentioned before, these fluctuations can be reduced by decreasing the slip speed deceleration at the region that close to engagement moment. Namely, reducing the oncoming clutch normal force before engagement. In Figure 5.6 simulation results of this strategy are shown.

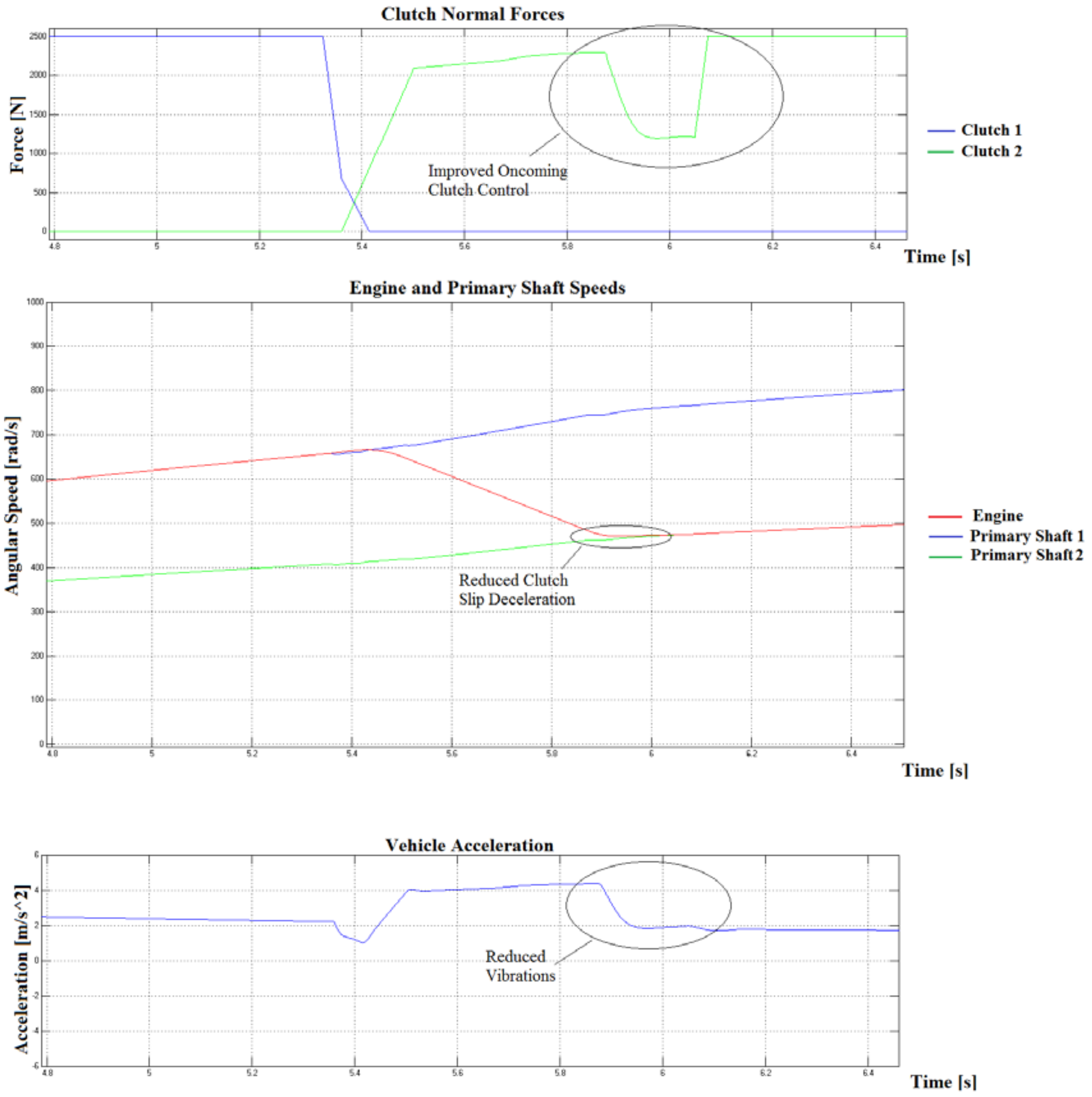

Figure 5.6 : Simulation results of 1-2 power-on upshift process with improved strategy.

Control of clutch slip at the vicinity of zero by the help of clutch normal force reduction can help to eliminate oncoming clutch engagement vibrations as can be seen in Figure 5.6.

5.2 Case 2

The second case starts with launch and acceleration under the condition of negative road gradient and very low APP input. Following these power-off upshifts up to 4th gear, rapid APP increment by driver due to gradient change from negative to positive value. This causes power-on downshift (from 4th to 3rd gear) in order to satisfy high torque demand. Afterwards power-on upshift (from 3rd to 4th gear) caused by acceleration with high APP and positive road gradient takes place. Finally, two sequent upshifts (from 4^{th} to 6^{th} gear) occurs due to rapid deceleration of APP.

Clutch input and output speeds, vehicle speed and acceleration and clutch normal forces of the case are shon in Figure 5.7:

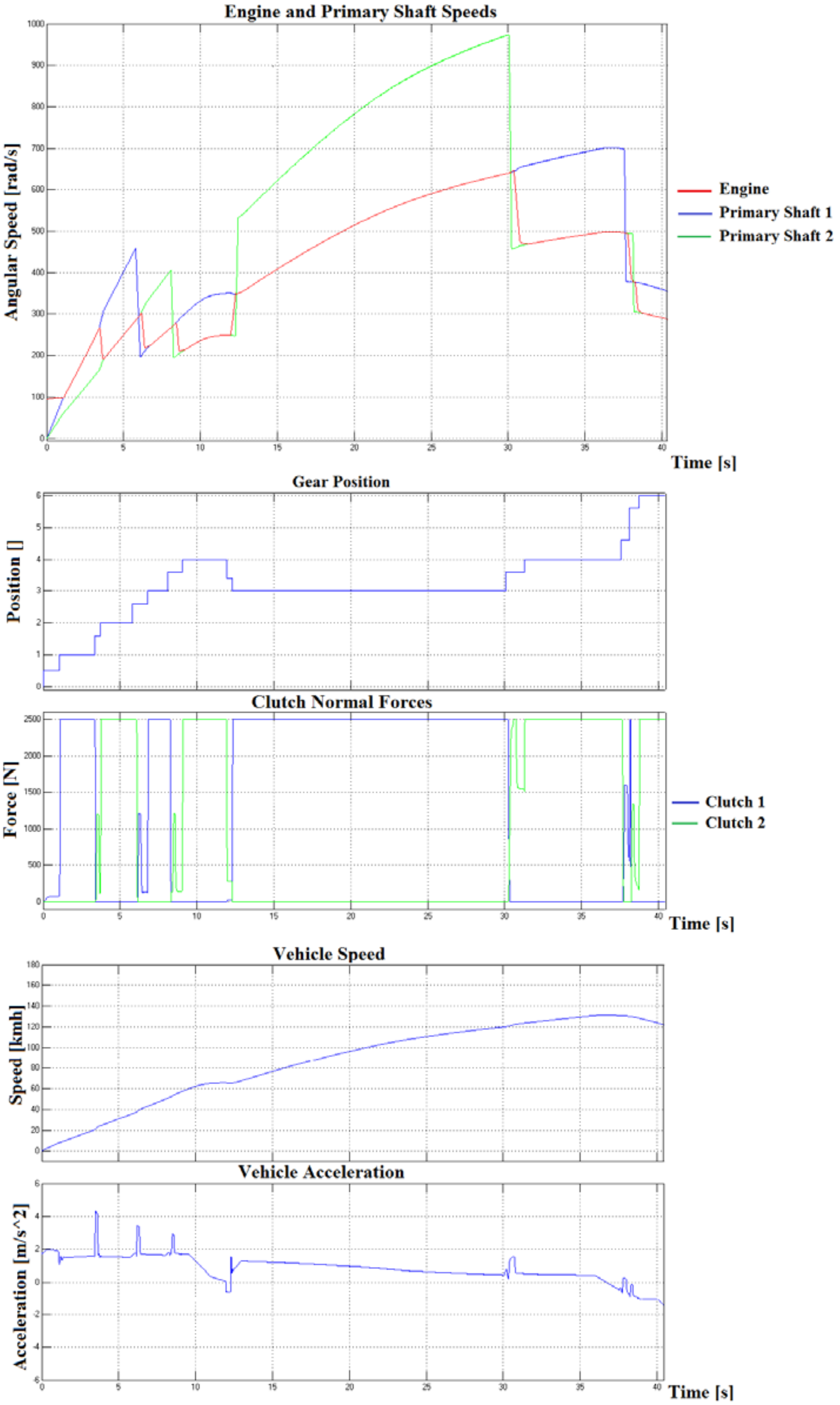

Figure 5.7 : Overall simulation result profiles of Case 2.

Launch process, 1-2 power-off upshift, 4-3 power-on downshift, 3-4 power-on upshift and 4-5, 5-6 sequent power-on upshifts are chosen to investigate more detailed.

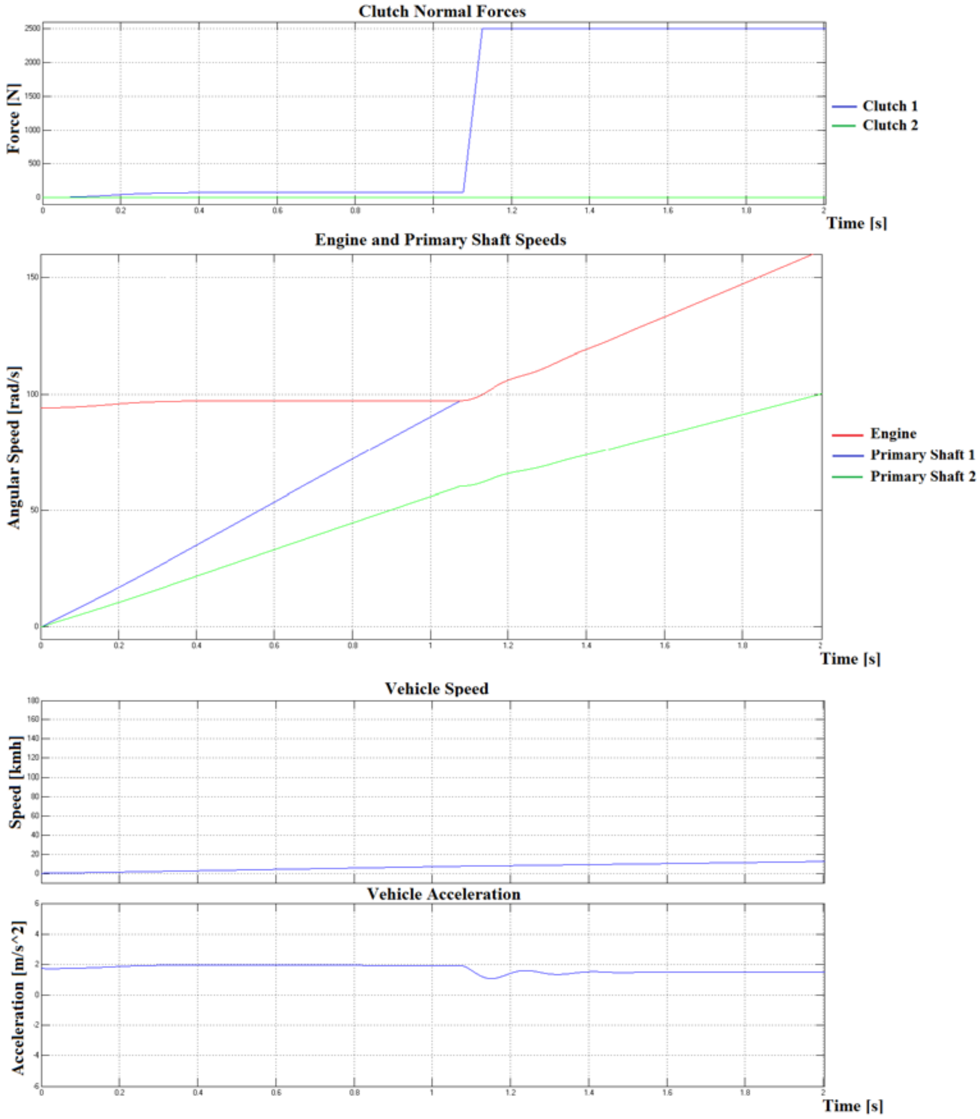

Figure 5.8 : Simulation results of launch process from Figure 5.7.

As can be seen in Figure 5.8, comparing with case 1, engine speed remain at lower target speed during launch process with %14 APP and -0.2 rad road gradient. And engagement fluctuations are also lower.

1-2 power-off upshift, occurred at the same conditions, is shown in Figure 5.9:

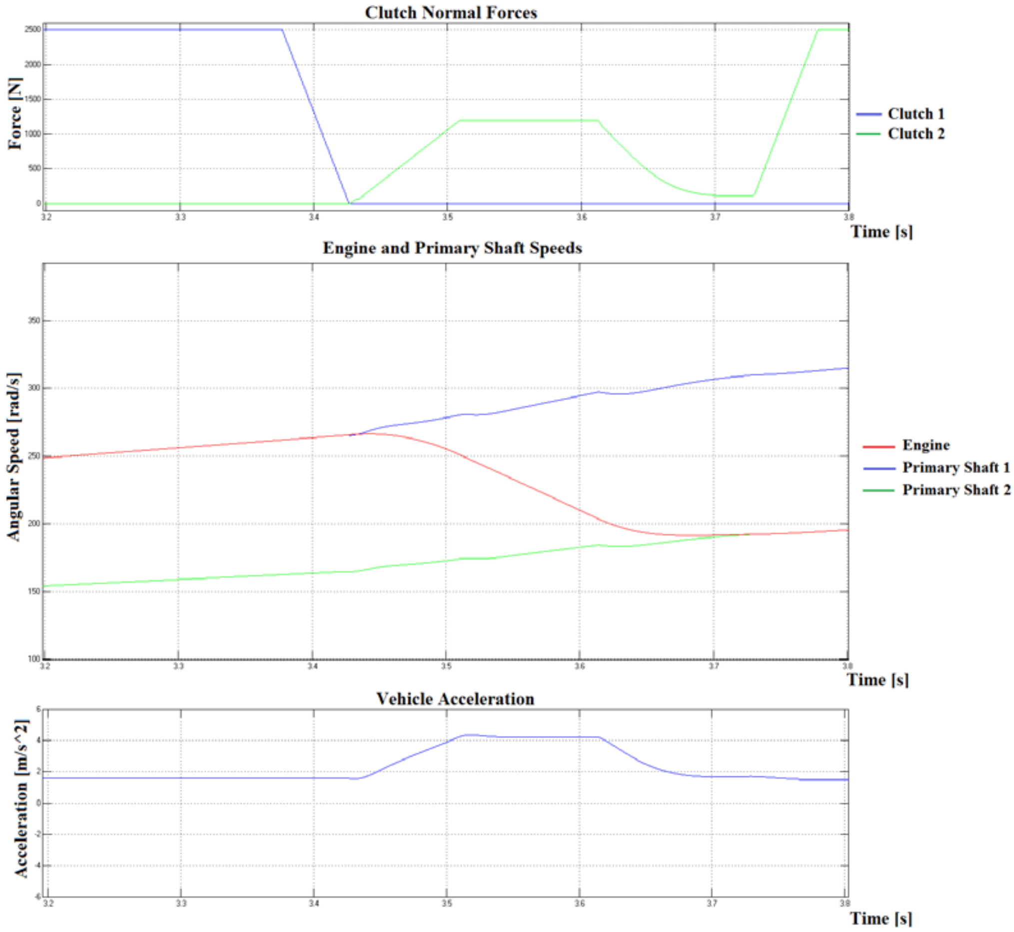

Figure 5.9 : Simulation results of 1-2 power-off upshift process from Figure 5.7.

As can be seen in Figure 5.9, during power-off upshift positive clutch slip region is not obtained unlike power-on upshift. Because there exists negative force throughout offgoing clutch before slip initiation. Namely, the engine and clutch input side is already in tendency to deceleration. Therefore, while offgoing clutch normal force decreasing, clutch slip starts with a negative value. This can cause negative torque when slip starts, however there exists no torque demand during power-off upshift processes.

Detailed graphs of power-on downshift under the condition of %90 APP and +0.22rad road gradient are shown in Figure 5.10:

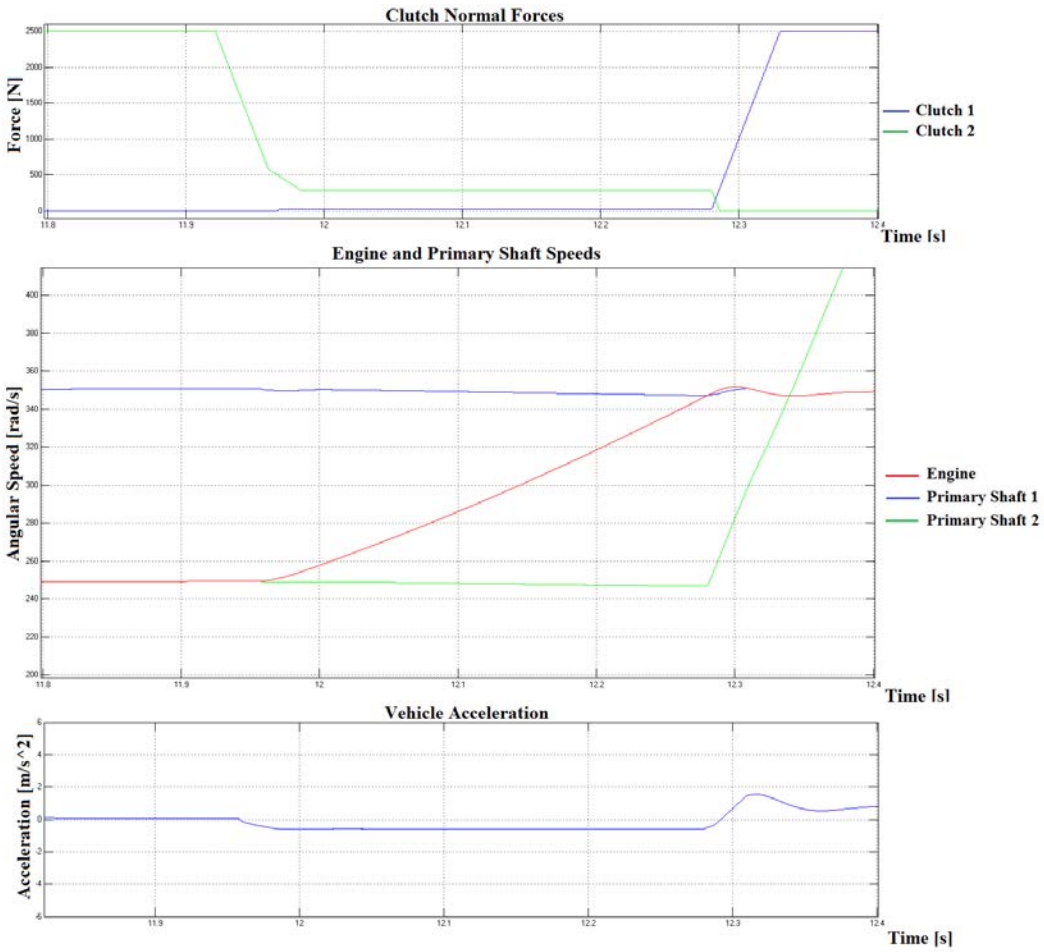

Figure 5.10 : Simulation results of 4-3 power-on downshift process from Figure 5.7.

During inertia phase (engine speed synchronization) of power-on downshift undesired negative vehicle acceleration is obtained (Above figure) as result of high positive road gradient. Although there exists no torque interruption, negative acceleration occurred due to torque hole caused by inertia phase.

And fluctuations after the engagement moment subsequent to positive clutch slip duration are caused due to high APP. Oncoming clutch engagement is executed during positive clutch slip region in order to ensure positive torque on oncoming clutch during power-on downshift. However, engine speed deceleration back to the oncoming clutch primary shaft speed caused fluctuations about the engagement moment.

In the following figure (Figure 5.11), simulation and experimental results are shown from different study (Liu, Qin, Jiang, Zhang 2014) with similar shifting strategies for 3-2 downshift. Afterwards the resuts will be compared.

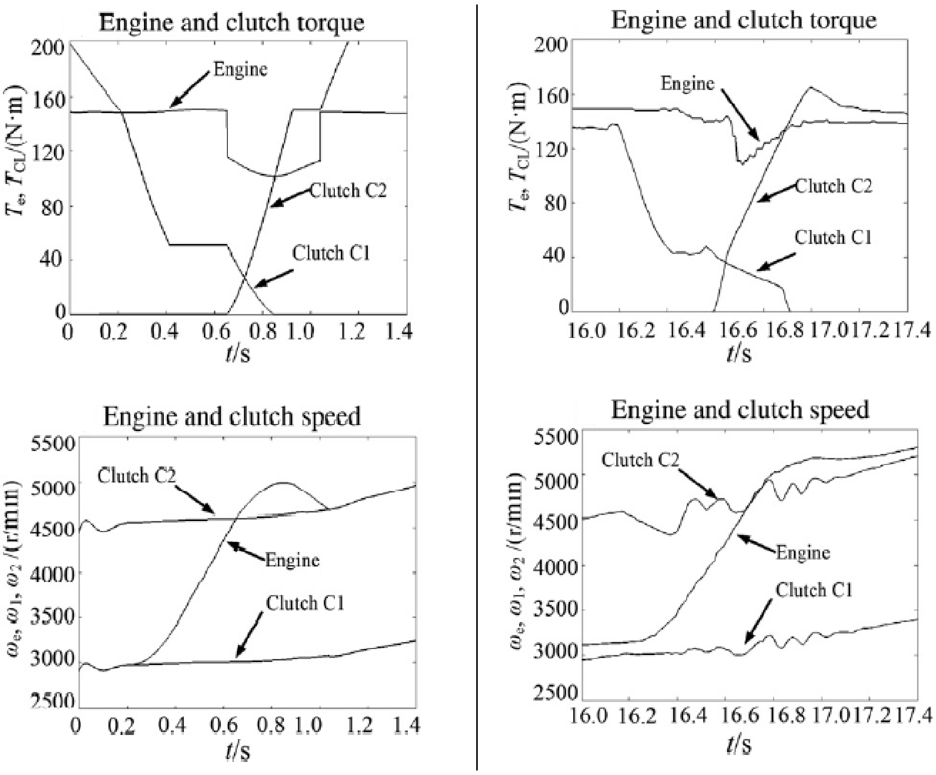

Figure 5.11 : Simulation and experimental results of 3-2 downshift process from different study (Liu, Qin, Jiang, Zhang 2014).

In the paper of (Liu, Qin, Jiang, Zhang 2014), similar shifting control strategies are used and simulation and experimental results are obtained as in the above figure. The offgoing clutch force is decreased and remain constant during inertia phase. By the end of inertia phase, offgoing clutch force is decreased and oncoming clutch force is increased simultaneously. Similar speed profiles and shift time with that of this thesis are obtained. Longer positive oncoming clutch slip region is obtained in (Liu, Qin, Jiang, Zhang 2014). However, positive clutch slip region in this thesis is long enough for torque phase to avoid negative clutch friction torque.

In Figure 5.12 power-on upshift under the same conditions (%90 APP and 0.22 rad road gradient) is investigated detailed.

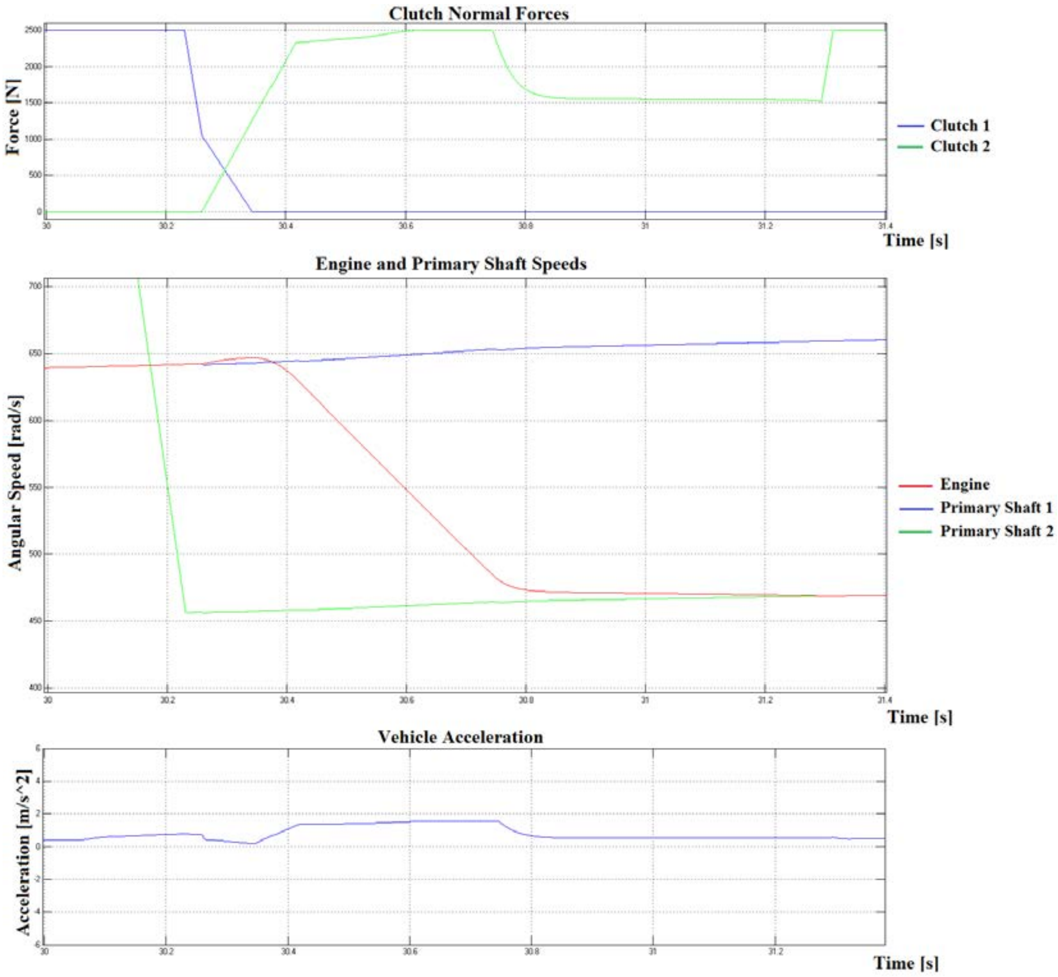

Figure 5.12 : Simulation results of 3-4 power-on upshift process from Figure 5.7.

3-4 power-on upshift is examined in the above figure. There exists positive clutch slip region at this power-on shift process as well. During inertia phase, oncoming clutch force is relatively high due to high APP. This caused high clutch torque and represented driver intention.

In the following figure (Figure 5.13) two sequent power-on upshifts (4-5 and 5-6) upshifts are investigated detailed. These shifts are initiated by APP decrease with high rate of change.

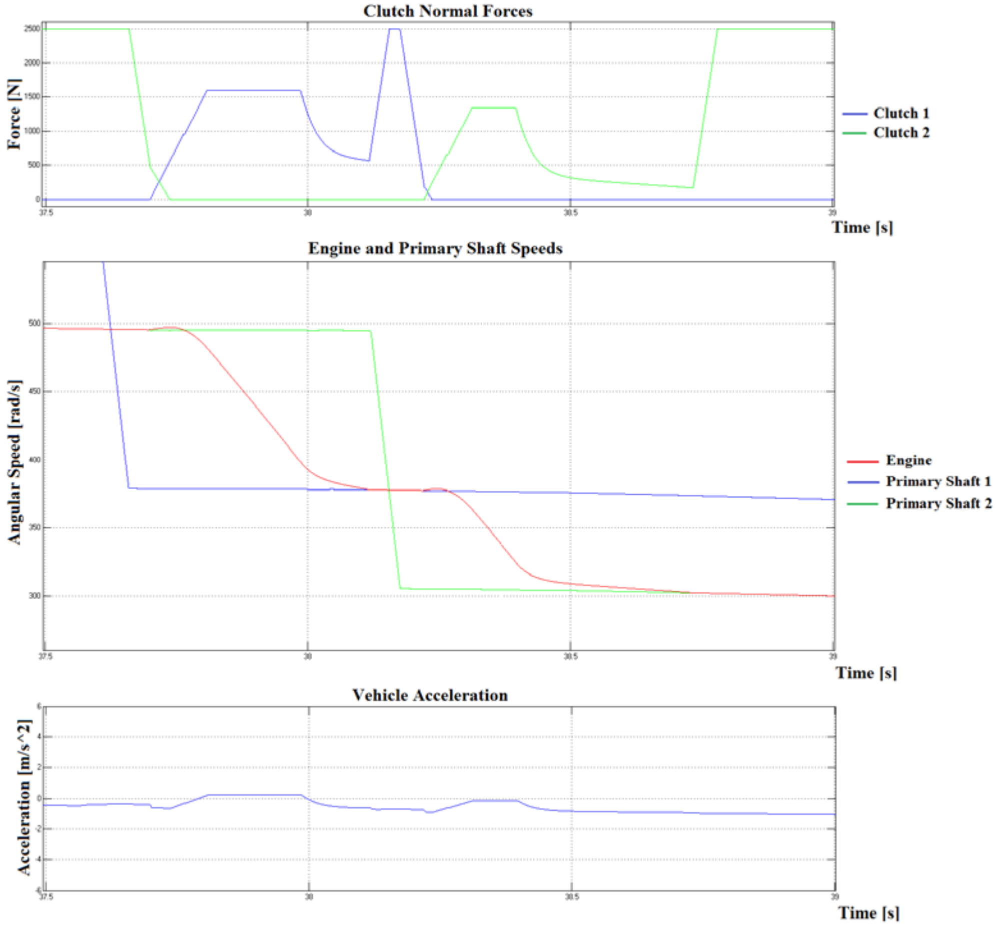

Figure 5.13 : Simulation results of 4-5 and 5-6 power-on upshift process from Figure 5.7.

For sequent shifts, shifting duration gains importance. Short shifting time provides quick response to the driver input. As can be seen in Figure 5.13, two shifting time is about 1.2 seconds including synchronizer operations which is a reasonable value.

5.3 Case 3

This case is determined in order to examine behavior of the transmission under the condition of rapid deceleration of the vehicle. This situation can cause engine flame out in case of long shifting time. Engine and transmission primary shafts speeds, vehicle speed and acceleration and clutch operations are shown in the following figure.

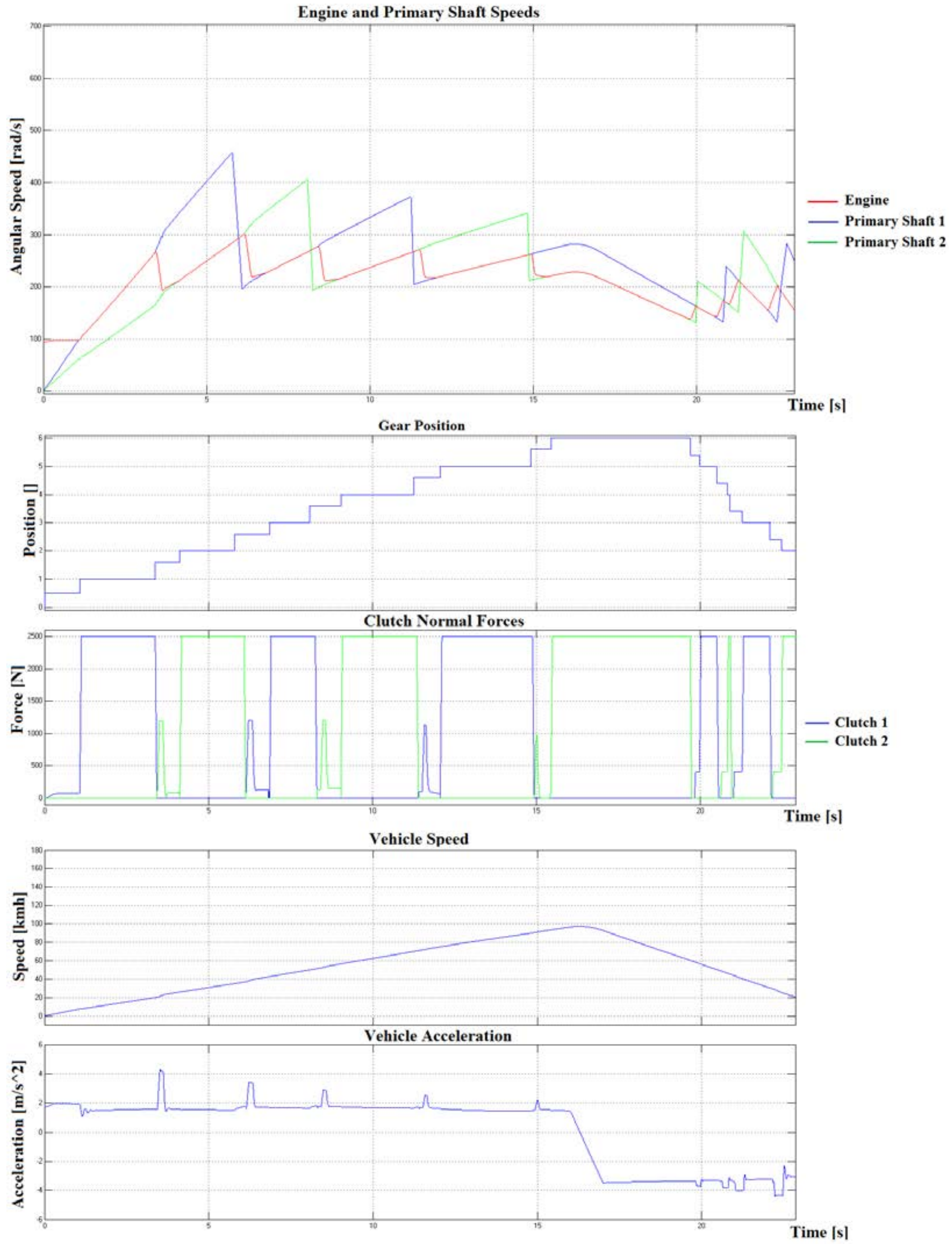

Figure 5.14 : Overall simulation result profiles of Case 3.

As can be seen in ‘Vehicle Acceleration’ graph, torque hole, clutch engagement fluctuations and shifting duration values of the lowest gear downshift are higher than that of the other downshifts due to higher gear ratio and higher primary shafts and clutch input-output speed difference. Hence, 3-2 downshift process is investigated in the Figure 5.15:

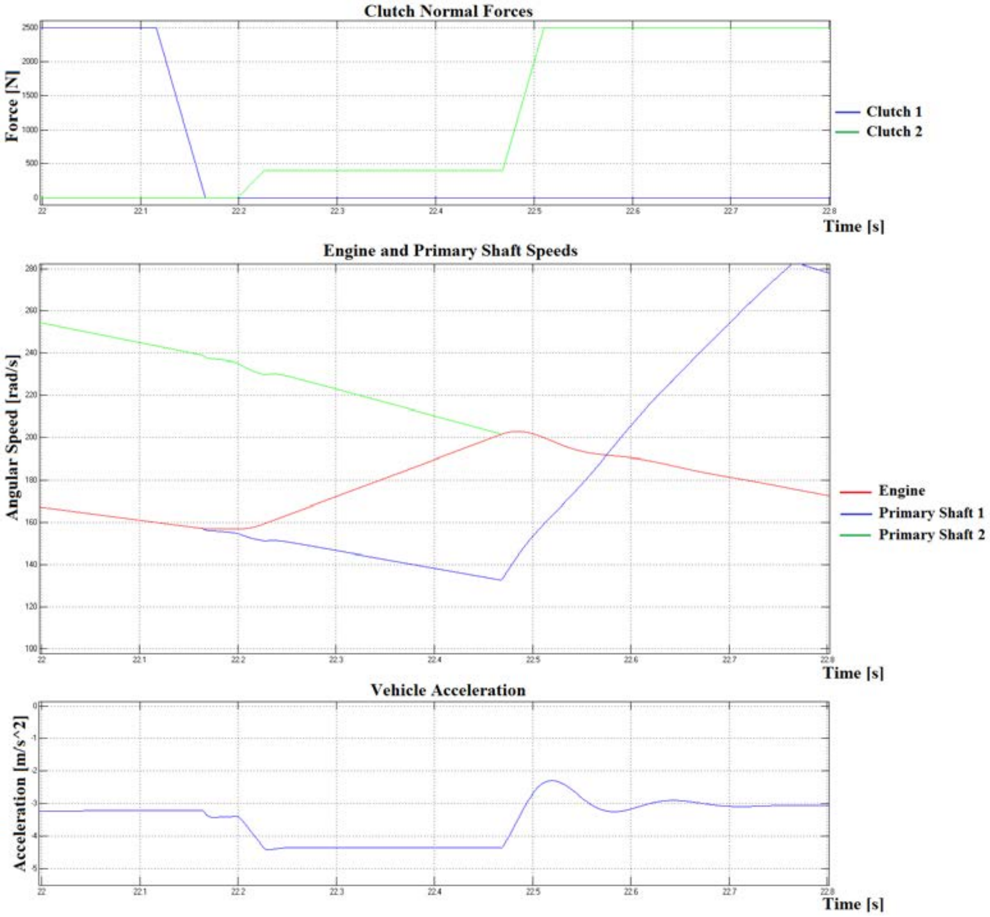

Figure 5.15 : Simulation results of 3-2 power-off downshift process from Figure 5.14.

Downshift process seen in Figure 5.14 is a power-off shift. Engine speed synchronization during inertia phase is realized by oncoming clutch. This cause negative clutch torque and torque hole during inertia phase which is expected for power-off downshift.

As a result, The mathematical model and gearshift control module are analized and examined by the help of various possible cases determined for a vehicle. Reasonable engine and primary shaft speed profiles and vehicle acceleration responses are obtained. Hence, the powertrain model can be considered representative for a powertrain with dual clutch transmission and used for further control strategy developments.

6. FUTURE WORK

In this study, mathematical modeling of a powertrain with dry dual clutch transmission is focused in order to use further gearshift control applications in the future. Some components of the model are considered more critical to be improved in order to obtain more accurate and representative model. Modular approach that used in this study provides convenience for progress the model in parts.

Improvements that should be done are specified as follows:

- A tire model based on tire slip should be modeled in order to obtain more realistic vehicle responses.
- Integrated control strategies should be adopted. Namely, engine manipulation should be used to avoid torque hole and torque hump during inertia phase.
- Clutch actuator model should be considered.
- More complex shift control strategies should be used on the purpose of shift quality improvement.
- Simulation speed should be increased.

REFERENCES

Berkel, K., Hofman, T., Serrarens, A. and Steinbuch, M. (2014). Fast and smooth clutch engagement control for dual-clutch transmissions. *Control Engineering Practice*, *22*, 57–68.

Deng, T., Hu, F., and Sun, D. (2012). Study on torque control strategy of dual clutch transmission during shifting. *Applied Mechanics and Materials* Vols. 121-126, 3541-3545.

Dolcini, P. J., Wit, C. C. and Béchart, H. (2010). Dry clutch control for automotive applications. Springer-Verlag London Limited, DOI 10.1007/978-1-84996-068-7

Ford-Werke GmbH. (2010). Servis egitim programları, D-F/GT1 (GB).

Goetz, M. (2005). Integrated powertrain control of twin clutch transmission. *PhD Thesis*, University of Leeds School of Mechanical Engineering.

Goetz, M., Levesley, M. C. and Crolla, D. A. (2005). Dynamics and control of gearshifts on twin-clutch transmissions. *Institution of Mechanical Engineers, Part D: Journal of Automobile Engineering, 951*, 1-14.

Kulkarni, M., Shim, T. and Zhang, Y. (2007). Shift dynamics and control of dual-clutch transmissions. *Mechanism and Machine Theory, 42*, 168–182.

Liu, Y., Qin, D., Jiang, H. and Zhang, Y. (2009). A systematic model for dynamics and control of dual clutch transmissions. DOI: 10.1115/1.3125883.

Liu, Y., Qin, D., Jiang, H., Zhang, Y. (2014). Shift control strategy and experimental validation for dry dual clutch transmissions. *Mechanism and Machine Theory*, *75*, 41–53.

Naunheimer, H., Bertsche, B., Ryborz, J. and Novak, W. (2011). Automotive transmissions. Springer-Verlag Berlin Heidelberg, Secon edition.

Ni, C., Lu, T. and Zhang, J. (2009). Gearshift control for dry dual-clutch transmissions. *WSEAS Transactıons on Systems.* Vol. 8, Issue 11, ISSN: 1109-2777.

Vigliani, A., Galvagno, E., Velardocchia, M. (2011). Dynamic and kinematic model of a dual clutch transmission. *Mechanism and Machine Theory, 46,* 794–805.

Walker, P. D., Zhang, N. and Tamba, R. (2011). Control of gear shifts in dual clutch transmission powertrains. *Mechanical Systemsand Signal Processing, 25,* 1923–1936.

Walker, P. D., Zhang, N. (2012). Engagement and control of synchroniser mechanisms in dual clutch transmissions. *Mechanical Systems and Signal Processing 26,* 320–332.

Walker, P. D., Zhang, N. (2013). Modelling of dual clutch transmission equipped powertrains for shift transient simulations. *Mechanism and Machine Theory, 60,* 47–59.

Zhang, Y., Chen, X., Zhang, X., Jiang, H. and Tobler, W. (2004). Dynamic modeling and simulation of a dual-clutch automated lay-shaft transmission. *American Institute of Physics*, DOI: 10.1115/1.1829069.

Zhao, Z.G., Chen, H.J., Zhen, Z.X. and Yang, Y.Y. (2014). Optimal torque coordinating control of the launching with twin clutches simultaneously involved for dry dual clutch transmission. *Vehicle System Dynamics: International Journal of Vehicle Mechanics and Mobility*, DOI: 10.1080/00423114.2014.902084.

Zhao, Z. G., Jıang, J. L., Yu, Z. P., and Zhang, T. (2013). Starting sliding mode variable structure that coordinates the control and real-time optimization of dry dual clutch transmissions. *International Journal of Automotive Technology*, Vol. 14, No. 6, 875−888.

Zhao, Z., Chen, H. and Yang, Y. (2014). Fuzzy determination of target shifting time and torque control of shifting phase for dry dual clutch transmission. *Mathematical Problems in Engineering*, Vol. 2014, Article ID 347490.

Url-1<*http://www.mathworks.com/help/physmod/simscape/ref/translationalfriction.html* >, date retrieved 18.05.2015.

CURRICULUM VITAE

Name Surname:	**Özgün BALCI**
Place and Date of Birth:	**İzmir/TURKEY, 06.04.1989**
E-Mail:	**obalci@yildiz.edu.tr**
EDUCATION:	**B.Sc.**
B.Sc.:	**2012, Yıldız Technical University, Mechanical Engineering**

PROFESSIONAL EXPERIENCE AND REWARDS:

2015, Research Associate, Yıldız Technical University